AFFIDAVIT

I declare that I have authored this thesis independently, that I have not used other than the declared sources/resources, and that I have explicitly indicated all material which has been quoted either literally or by content from the sources used. The text document uploaded to TUGRAZonline is identical to the present master's thesis.

_____
Date

_____
Signature

IEBW

Ballast Evaluation as Part of Tamping Measures

Master´s Thesis

Submission March 2019

Stefan Offenbacher
BSc
01330203
stefan.offenbacher@tugraz.at

Supervisor:
Matthias Landgraf
Dipl.-Ing. Dr.techn.
m.landgraf@tugraz.at

Second supervisor:
Johannes Neuhold
Dipl.-Ing. Dipl.-Ing.
johannes.neuhold@tugraz.at

▸ www.ebw.TUGraz.at

Acknowledgements

Abstract

In combination with rails and sleepers, track ballast forms the superstructure of most railway lines. Its condition is influenced by many factors, e.g. cumulated tonnage, and therefore varies heavily. Poor ballast condition combined with high loads of train operation almost always causes issues with track geometry. These are generally met by lifting, realigning and tamping the respective sections.

This master´s thesis deals with data measured during such track works. Sensors mounted on tamping tines record different parameters. These are compared with prevailing ballast condition, known from other evaluation methodologies. As the tamping tines come in contact with the ballast bed during the tamping process, the measurements are expected to reflect its current condition. These findings can provide additional information for infrastructure managers who need to know the state of their network. Furthermore, these data enable optimization of tamping machine settings in consideration of different ballast conditions. Eventually, condition based tamping processes will be possible, with machine settings automatically adjusting to current ballast condition. This should improve track quality and sustainability of maintenance works.

The analyses of this study provide evidence of a connection between ballast condition and tamping machine recordings. Although further surveys using more data to erase any uncertainties are advisable, the possibility to determine ballast condition with tamping machines and modify settings accordingly, exists.

Kurzfassung

Die meisten Bahnstrecken weltweit werden mit Schotteroberbau ausgeführt, bestehend aus Schienen, Schwellen und dem Gleisschotter. Der Zustand des Gleisschotters wird von vielen Randbedingungen, wie zum Beispiel der kumulativen Verkehrsbelastung, beeinflusst, weshalb er netzweit starken Schwankungen unterliegt. Dieser Zustand beeinträchtigt seinerseits die Gleislagequalität maßgeblich. Verschmutzer Bahnschotter führt in Kombination mit hohen Achslasten von Zügen zwangsweise zu einer Verschlechterung der Gleisgeometrie. Um sicheren und reibungslosen Betrieb gewährleisten zu können, muss daher von Zeit zu Zeit eine Korrektur der Gleislage vorgenommen werden. Dieser Instandhaltungsprozess inkludiert Heben, Richten und Unterstopfen des Gleisrostes, um ein definiertes Schwellenauflager wiederherzustellen.

Im Zuge dieser Masterarbeit werden Messdaten analysiert, die während Stopfeinsätzen von mit Sensoren ausgestatteten Stopfpickeln aufgezeichnet wurden. Auf Grund des direkten Kontakts zwischen Stopfpickel und Gleisschotter wird ein Zusammenhang zwischen den gemessenen Parametern und der Schotterverschmutzung angenommen. Anschließend werden die Daten mit dem Schotterzustand auf den bearbeiteten Streckenabschnitten, welcher mittels valider Methoden evaluiert wurde, abgeglichen. Sind Zusammenhänge erkennbar, können die gewonnenen Kenntnisse in Zukunft einerseits zusätzliche Informationen für Infrastrukturbetreiber liefern und andererseits dazu verwendet werden, den gesamten Stopfprozess weiterzuentwickeln, beziehungsweise für unterschiedliche Schotterzustände zu optimieren. Auch eine automatische Adjustierung von Stopfparametern entsprechend dem aktuell erfassten Schotterzustand und eine damit einhergehend bessere und nachhaltigere Gleislagequalität soll damit ermöglicht werden.

Die Ergebnisse dieser Studie zeigen eindeutig, dass eine Korrelation zwischen den aufgezeichneten Messwerten und Schotterzuständen besteht. Dennoch sind weitergehende Analysen, basierend auf einer größeren Anzahl von Stopfeinsätzen und damit größeren Datenmengen, empfehlenswert, um Unsicherheiten und Schwankungen in den verwendeten Daten zu eliminieren.

Table of Contents

Table of Figures

1 Introduction, Structure and Aim

1.1 Introduction

From an economic point of view, transportation is a precondition for prosperity and economic growth of humans, businesses and countries. From a social and environmental perspective, the entire transportation sector goes along with numerous downsides: noise and air pollution adversely impact human health, oceans get contaminated, commuters are stuck in traffic jams every day and people get insured or even fatally harmed in accidents. This list could easily be continued. These aspects eventually result in high economic costs for society. Hence, transportation cuts both ways – it is a premise for affluence and origin of many (financial) drawbacks.

However, there are possibilities to enhance the transport sector. Many trips are avoidable in the first place, for example by applying smarter and more sustainable land use planning ("city of short distances"[1]) or giving preference to digital communication over physical meetings (especially in businesses). The remaining traffic needs to be handled in a way that ensures as little detrimental impacts on humanity and environment as possible. Having the downsides of transportation in mind, emphasising railways appears to be a smart approach towards a more sustainable future of transportation. Provided that renewable energy is used to power the trains, electrical rail transport is an environmentally friendly means of conveyance. As their operation is organized and permanently monitored, railroad cars cannot jam (under normal circumstances) and are safer than other systems too. These and other advantages induce policy makers to foster rail transport. In combination with ever increasing overall transport volumes, utilization of railway networks is steadily growing.

Besides the positive effects of emphasizing rail transport, a downside for its infrastructure comes along. More trains cause more wear of the track, thus increasing demand for inspection and maintenance. At the same time, required track closures for such tasks will become even more limited since railway operators seek to run their trains regularly and punctual, without interruptions. These permanently tightening boundary conditions require a continuous improvement of the system railway, from a sole track component to the complete network, from small inspection tools to the entire rolling stock. One part of this ongoing progress is improvement of track machinery, which this master´s thesis addresses. It investigates, whether data recorded during tamping actions allow conclusions about track condition and how these data can help improve achievable quality of work. It

---

[1] For more on *city of short distances*: http://www.oecd.org/cfe/regional-policy/50524895.pdf [22/12/2018]

is seen as a little contribution to the continuous enhancement, which is essential for the system to be prepared for the future.

1.2   Aim and Structure

Plasser & Theurer Export von Bahnbaumaschinen Gesellschaft m. b. H., an Austrian manufacturer for rail track maintenance and track laying machines, have equipped tamping tines of one tamping machine with multiple sensors. These sensors record various parameters during each tamping process and are expected to deliver information about ballast condition. Preconditioned that the measurements are meaningful, the data provide several opportunities:

- The understanding of ballast behaviour and the influence of contamination can be improved.
- Infrastructure managers get additional information for maintenance planning.
- Tamping equipment and tamping machinery settings can be improved and adjusted to varying ballast conditions to deliver even higher and more sustainable track quality.

In this master´s thesis, a first set of measurement data recorded during tamping actions in 2016 and 2017 is analysed. Simultaneously, ballast condition of the tamped sections is evaluated with proven, adequate methods. These two datasets are then connected and examined for correlations between measurement data from the tamping machine and ballast condition. The study aims to answer the following questions:

1. Can a link between ballast condition and the recorded measurements be established?
2. Are data recorded during tamping processes suitable to accurately assess ballast condition?
3. Besides ballast condition, are there other factors that influence the recordings?
4. Which of the measured parameter(s) is (are) most suitable for ballast condition evaluation?

To answer these questions, a well-structured approach is chosen. As the overall aim of this work is to create a link between the two topics of *ballast condition* and *tamping*, the first big part of this study provides background information about these subjects. It is divided into two chapters, beginning with track ballast. Among the discussed issues are the functions of the ballast bed, the relevance of its condition and how it can be evaluated. Next, tamping actions are investigated, including their purpose, a historical overview and a detailed description of the process.

The second great part is devoted to data analyses, starting with an explanation of the two utilized data sources – recordings from the tamping machine on the one hand and information of the Austrian railway infrastructure on the other. Afterwards, the process of preparing the required data and connecting the two data sets is described. Subsequently, the essential analyses and results are presented, divided into a chapter discussing general outputs and a second one focusing on ballast condition assessment. The final pages are intended to summarize the quintessence, accentuate possible uncertainties and give an outlook for the future.

Unless stated otherwise, technologies, threshold values and other specifications which are mentioned, refer to Austrian standards (which are similar to railway affine countries in and outside Europe).

2 Track Ballast

Track ballast is an essential component of (most) railway lines. It serves multiple purposes and is subject to strict requirements. In this study, the emphasis is put on ballast condition and how to monitor it. To underline the importance of the ballast bed, the functionality of railway tracks, in general, is explained beforehand.

2.1   Superstructure

Although most railway tracks may look similar, they can differ in many details. One of the most prominent is the type of superstructure. Superstructure must absorb all vertical, longitudinal and lateral forces arising from static and dynamic loads during train operation. These forces must be channelled to the substructure in a way that guarantees safe operation and long service life of the track and all its components. Figure 1 shows, how the pressure in the small rail-wheel contact area is steadily reduced within the superstructure. At the bottom, the pressure level is low enough for the substructure to withstand it.
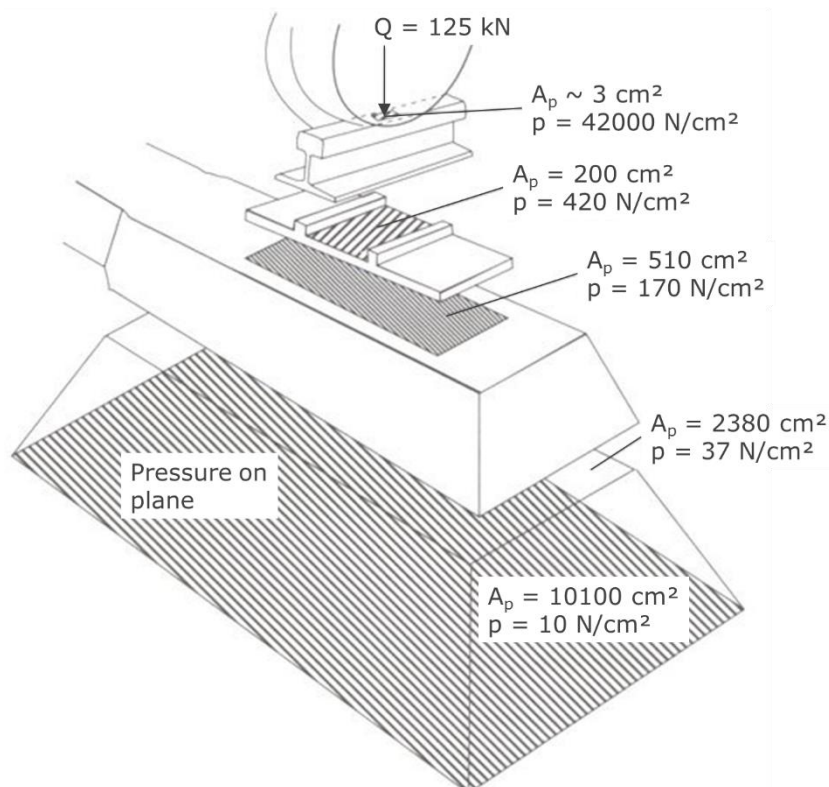
Figure 1: Pressure reduction within track structure acc. to [1]

Over the years, two main types of superstructure have proven to be effective for standard gauge railway systems: ballasted track, which has been used for centuries, and slab track as an answer to ever higher demands.

As this master´s thesis merely applies to ballasted track, it is the only system of interest for this study. Nevertheless, for the sake of completeness, a short introduction to slab track is given below, pointing out the advantages and disadvantages compared to ballasted track.

2.1.1 Slab Track

Steadily growing demands for railways require the infrastructure to evolve. Especially the ever-growing speeds show the limits of conventional track structure. Trains running over 250 kilometres per hour may whirl stones of the ballast bed and damage the rolling stock. Furthermore, the velocity of vertical vibration within the infrastructure rises significantly with increasing speed, hence track alignment deteriorates quickly. [2]

To counteract these problems, slab track systems were developed. Instead of bedding sleepers in a ballast bed, concrete frames or concrete slabs are directly placed on the formation. [3] Slab tracks meet very high requirements concerning track alignment, which is particularly important on high-speed lines. Without ballast, which is frequently a limiting component, these systems also need less maintenance and can reach higher life spans. Despite the advantages, slab tracks are not the most commonly used system, due to some inherent drawbacks: Installation of slab track is more expensive and the high initial invest-ment costs bear deterrent effects. Another issue is the lack of continuity in track work. [4] While conventional tracks are laid, maintained and renewed by continuously working ma-chines, work on slab track is less mechanized. Thus, maintenance (e.g. in case of a derail-ment) and track renewals last longer and costs for operational hindrances are higher. Ad-ditionally, track geometry can only be corrected to a certain degree. If settlements exceed a threshold limit, expensive measures like ground injections are required. For these rea-sons, slab tracks are mainly installed on high speed lines as well as on bridges or in tunnels (where settlements are impossible to a great extent). [3]

As slab tracks do not feature ballast beds, they cannot be tamped. Therefore, they are irrelevant in the further course of this study.

2.1.2 Ballasted Track

Ballasted tracks have been implemented and enhanced since the first big boom of railways at the beginning of the 19th century. As for its versatility, it is still the most extensively used system in the world. [2] Ballasted track primarily consists of three components: rails, sleepers and ballast (Figure 2). In addition, smaller parts like rail pads and fastenings are part of ballasted superstructure too.
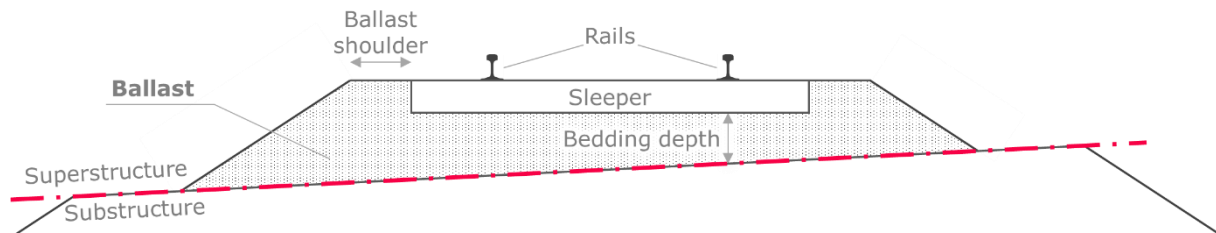
Figure 2: Cross section of ballasted track

Regarding structure and functionality, all ballasted tracks are equal. However, they vary in several details such as rail profile, sleeper material or type of rock of the ballast bed. Rails are available in different shapes and chemical compositions, but they are not of concern and, therefore, not dealt with in this study. Sleepers differ in terms of general structure (e.g. conventional sleeper vs. frame sleeper), dimensions and material. Conventional wooden or concrete sleepers are the main types used in Austria. Table 1 reveals some of their pros and cons, which also define applicability under certain conditions.

	Wood	Concrete
Advantages	little weight high elasticity (protects ballast from impact effects) easy to exchange	low costs insensitive to environmental conditions high life span
Disadvantages	limited life span sensitive to environmental conditions more expensive than concrete	little elasticity sensitive to impact effects (generally need to be exchanged in case of derailment) heavy (hampers manual exchange)

Table 1: Comparison of sleeper types acc. to [1]

More recent developments are concrete sleepers with an elastic layer (under sleeper pad, USP) at the bottom. This combines advantages of concrete sleepers (e.g. high life span, high resistance to environmental conditions) with advantages of wooden sleepers (e.g. attenuation of impact effects and protection of the ballast bed) [5], [6]. Concrete-USP sleepers demand less maintenance and extend service life of track [7]. This implicates an economic advantage, which makes the system advisable for new lines. Moreover, concrete-USP sleepers should also be installed during track renewals on medium to highly loaded lines. The financial benefit of this sleeper type ensures that more and more sections in Austria will be equipped with this system. [8]

On a ballasted track, the track grid is embedded in rock particles. Under adequate conditions, this ballast bed fulfils essential tasks [9]:

- It distributes arising loads evenly from the sleepers to the substructure.
- It provides elastic properties to minimize dynamic forces.
- It secures sleepers in their position.
- It enables easy recovery of track alignment.
- It guarantees permeability of water and air.

These tasks demand very strict requirements for ballast. Hence, not every material is suitable. Wear-resistant hard stone like basalt, granite, diabase, granulite or similar are favoured. Furthermore, grain size distribution is of great importance to provide the desired properties concerning load distribution, elasticity and permeability. Only if mechanical and geometrical requirements are met, the ballast can be used. [9]

2.2   Elasticity and Load Distribution of Ballasted Track

One inherent property of railways is that they are a mass transport system. This implicates the generation of huge forces beneath the wheels of railroad cars. Static loads reaching 22.5 tons per axle (225 kN), increased by up to 25 % through dynamic effects, are very demanding for the track. Heavy haul lines in other countries even exceed these values. If the entire load was induced at a single point, track components would quickly wear and eventually fail. Only a distribution of these forces ensures reasonable lifespans of the components. This is achieved by allowing rails to bend in vertical direction. Through this effect, the arising forces are spread over a longer segment and about five to nine sleepers share the load (Figure 3). [1]
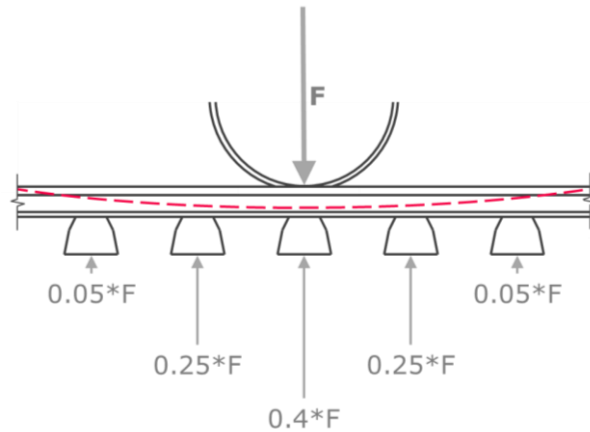
Figure 3: Force apportionment through vertical compliancy acc. to [1]

Only elasticity within the track structure enables the rails to form a deflection curve under load and return to the initial position afterwards. All track components along the force path offer elastic behaviour to a certain degree and depending on their condition. The biggest contributor is substructure, providing about 40 % of overall track elasticity. Ballast itself accounts for about 20 to 25 %. Figure 4 depicts a complete compilation of involved components and how much they contribute to overall track elasticity. As illustrated, however, it depends not least on component choice. [1]
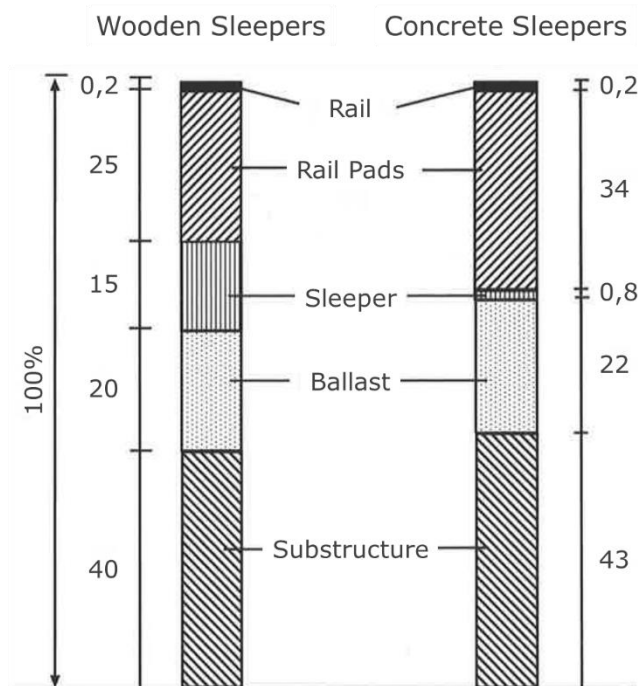
Figure 4: Contribution of components to overall track elasticity acc. to [1]

The origin of ballasts' elastic behaviour lies within its structure. New ballast consists of rough-edged rocks with common grain sizes between 31.5 and 63 millimetres.[2] This grain size distribution ensures that vacant space remains between the interlocked rock particles.

---

[2] Category GC RB B of EN 13450

This, in turn, enables redistribution of grains through rotation, translation and gliding of the particles. To a large degree, this process is reversible and can therefore, in simplified terms, be interpreted as elastic behaviour. [10]

Vertical compliancy of track guarantees that every sleeper only receives a fraction of the entire load. Nevertheless, the pressure at the bottom of the sleepers would still be too high for the substructure. The ballast bed, however, disperses the load over a larger area. This reduces the pressure to acceptable levels. For best possible load transfer, an even pressure on substructure would be ideal [9]. A realistic pressure distribution on the ground, resulting from one axle, is demonstrated in Figure 5.
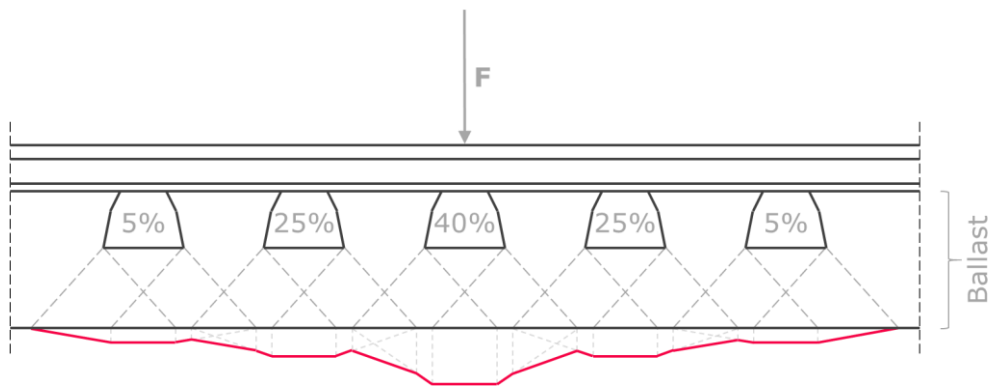
Figure 5: Pressure on formation acc. to [9]

Assuming a load distribution angle of 42 degrees and a sleeper gap of 60 centimetres, the optimal ballast depth for uniform substructure pressure would be 30 centimetres [9]. However, smaller angles of about 20 degrees are more common under real conditions [11]. Thinkable solutions would be a deeper ballast bed or a shorter sleeper gap. Results of too little ballast depth combined with a narrow load distribution angle are shown in Chapter 2.3.3

2.3   Ballast Fouling

Ballast is subject to wear and is exposed to contamination over time as well (Figure 6). This can have several causes and effects, all of which share the same adverse outcome: the ballast bed loses its desired properties and eventually track alignment issues arise.
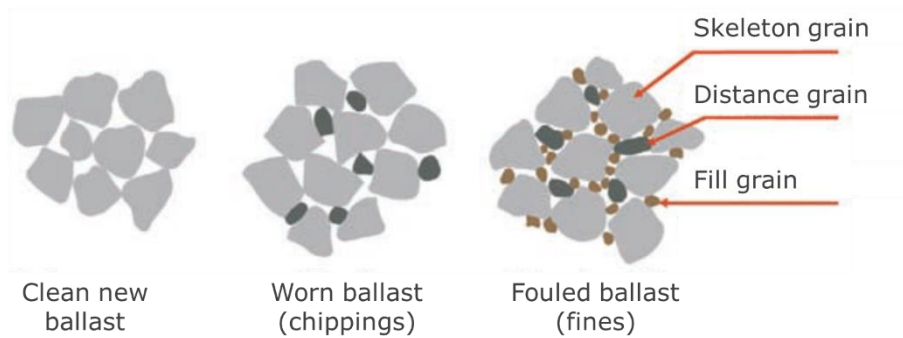
Figure 6: Ballast states acc. to [12]

Fine grains accumulating between the ballast stones is called *ballast fouling*. It worsens load distribution in the bedding and hampers dewatering. Thus, strength and elasticity of the bedding decline. Possible origins of these fines are described below.

2.3.1 External Input

When constructing or renewing tracks, ballast can contain a small amount of fine grains. What is more, all sorts of particles are blown in by the wind, depending on how much the track is exposed to such kind of pollution. Another problem, especially on lines heavily frequented by trains shipping coal, gravel, wood or similar, is fouling caused by operation. Particularly older freight wagons tend to leak and disperse small particles directly into track. [12]

2.3.2 Train Operation and Maintenance

The rolling movement of a wheel causes the following sleeper to slightly take off while approaching, and then abruptly pushes it onto the ballast surface when running over it. Strain peaks in the small contact areas of the stones (see Figure 6 – Clean new ballast), emerging from these sudden impacts, can exceed rock strength. Chips or even cracked stones occur. Numerous grain redistributions during train passage cause abrasion too. Both effects round the rocks and increase the amount of fine grain in the ballast bed. Such ballast wear is particularly high at locations of changing substructure stiffness, e.g. the transition between free track and a bridge. In some cases, the stiffness change downright crushes the stones. [10] Maintenance actions, especially tamping (Chapter 3), also stress the rocks and abrade or crack them [12].

2.3.3 Substructure Particles

Small particles, fines and humidity can also infiltrate the ballast bed from underneath. The track profile in Figure 2 (page 6) shows an inclination of the substructure, intended to guide water off the track. On improper spots, water pockets can occur below the ballast. Then, vertical compression and relaxation during train passage generate pumping effects. This causes particles of the substructure to rise into the ballast bed. Lacking drainage next to the track accelerates this process. [12]

A similar effect is possible without dewatering issues too. If strain on the ground is irregular, for example resulting from insufficient bedding depth or a too small load distribution angle of the ballast, particles are squeezed up in areas of lower pressure (Figure 7). Particularly organic and compact soil are affected by that process. [12]
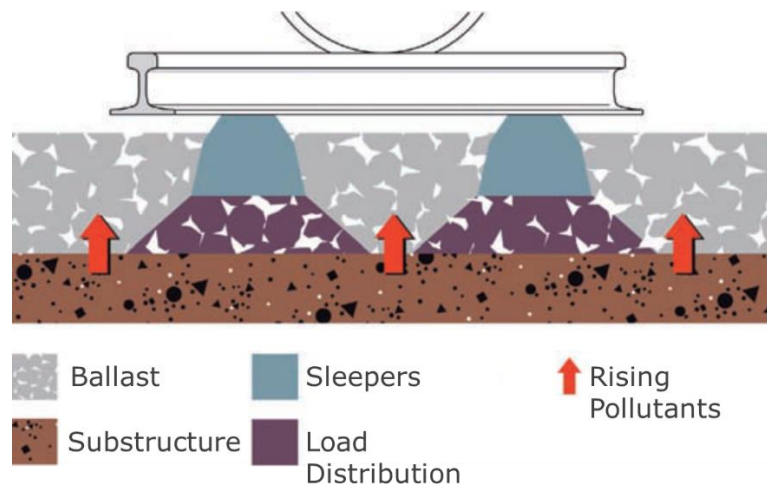
Figure 7: Irregular pressure on substructure acc. to [12]

In case of fouling ballast, a downward spiral occurs, regardless of the origin of the contaminant. Dewatering worsens, shear strength of the ballast bed decreases, load distribution changes and ballast stiffness increases. Less elastic and more plastic deformation causes track settlements. Subsequent alignment issues are often corrected by tamping the section (see Chapter 3). If ballast fouling has progressed to a severe degree, this maintenance just shows temporary rectification. Only ballast cleaning, maybe accompanied by substructure enhancements, sustainably solves the root cause of the problem. This extensive track work cannot be done during few traffic-free night hours. Instead, temporary track closures with all their consequences (rerouting of freight trains, rail replacement bus service for passengers) are required. When the track is shut down and train operation organized differently, it is reasonable to conduct as many works as possible in the blocked section. This means fouled ballast frequently triggers complete track renewals, which often makes it the limiting component for track service life.

2.4   Evaluation of Ballast Condition

The relevance of ballast condition calls for ways to monitor it. Only if the condition is known, decision-makers can determinate sustainable track maintenance. Several condition assessment methodologies are used in Austria, two of which will later be used for evaluations; they are introduced below. Besides them, geotechnical surveys like test excavations or cone penetration tests deliver detailed information about ballast and substructure condition. However, these are local investigations rather than regular, net-wide analyses and therefore less suitable for this study.

2.4.1   Ground Penetrating Radar

Ground penetrating radar (GPR) is a geophysical measurement system based on electromagnetic pulses. It enables non-destructive assessment of ballast- and substructure condition. Two antennas, one emitting and another recording electromagnetic signals, are mounted on the vehicle. The emitted pulses are reflected by targeted objects. As different materials offer different resistance to electromagnetic waves, the reflected signals deviate from the emitted pulses. These variations enable evaluations of the observed areas. Plotting the reflected signal as a function of amplitude and time and applying a colour code creates a radargram as presented in Figure 8. [13]
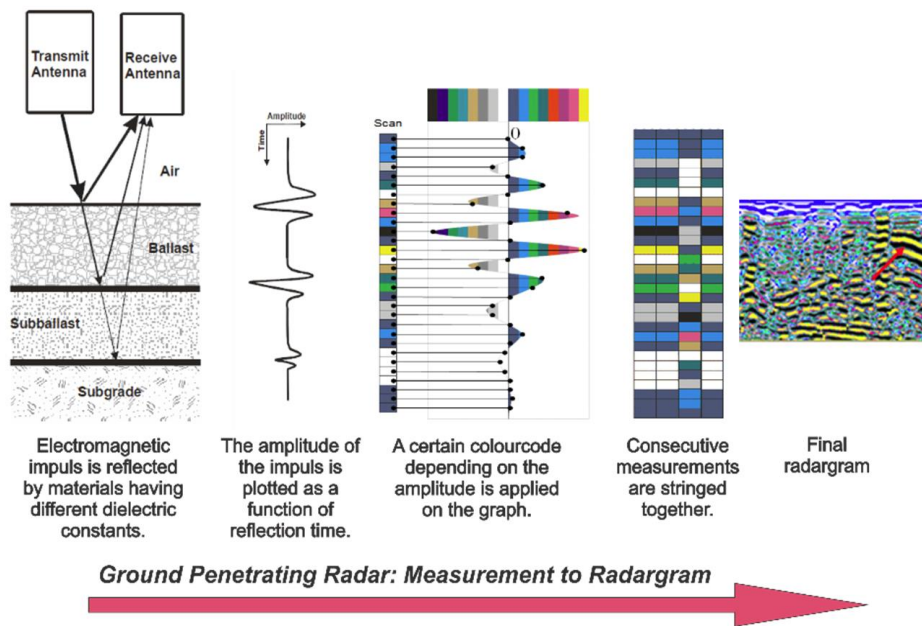
Figure 8: Creation of a radargram using GPR [13]–[16]

For better interpretation of GPR measurements, indicators have been developed to obtain easy-to-read outputs. The GPR results are divided into categories like *Ballast Fouling* or *Interlayer Humidity* and then classified (Figure 9). For example, *Ballast Fouling* can take five different states, from *Clean* to *Strongly fouled*. [17]
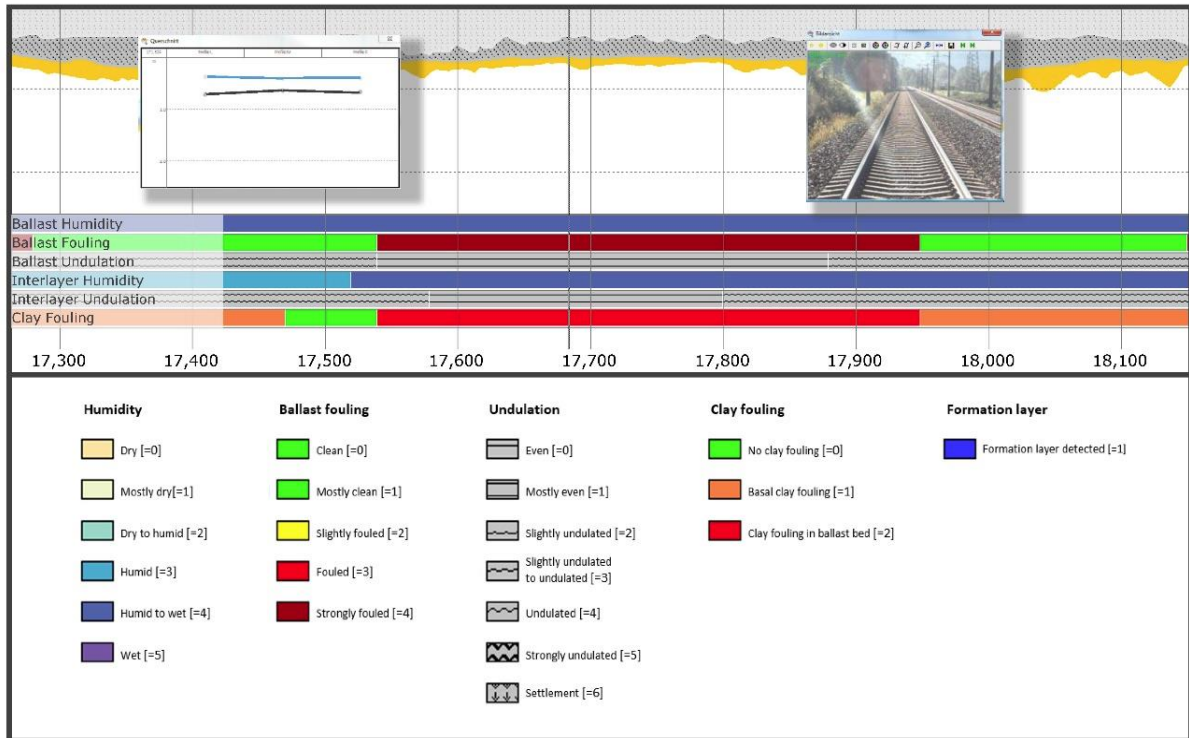
Figure 9: Representation of an ÖBB GPR analysis [17]

In Austria, ground penetrating radar has been used for track condition evaluation since 2012. Over the years, approximately 1.700 kilometres of the Austrian core network have been evaluated, providing valuable insight into ballast- and substructure condition on the main lines. [17]

2.4.2 Fractal Analysis

Another way to gain information on ballast- and substructure condition is a mathematical approach. Although it is very different, the method shares some properties with ground penetrating radar: both are indirect, non-destructive evaluations that can be conducted at high speeds (over 100 kph and up to 250 kph for ground penetrating radar and track monitoring car respectively). [17]

Fractal analysis for track condition is based on vertical track geometry, which in Austria is regularly evaluated by a track recording car. Conventional analyses of the vertical align-ment-signal, focusing on amplitudes of the signal, show irregularities in the track geome-try, but do not reveal the origins of errors. Hence, counteractive measures may not treat

the underlying problem. The fractal algorithm described below dissects the signal and analyses different wavelength ranges. This enables accurate conclusions about issues in the super- or substructure and identifies the root cause of the alignment irregularities.

At the beginning, a data segment of 150 metre length is subdivided into equal sections λ and the length of the resulting polygon L(λ) is determined. When the section length λ is progressively shortened, the polygon L(λ) converges towards the original signal (Figure 10). [18]
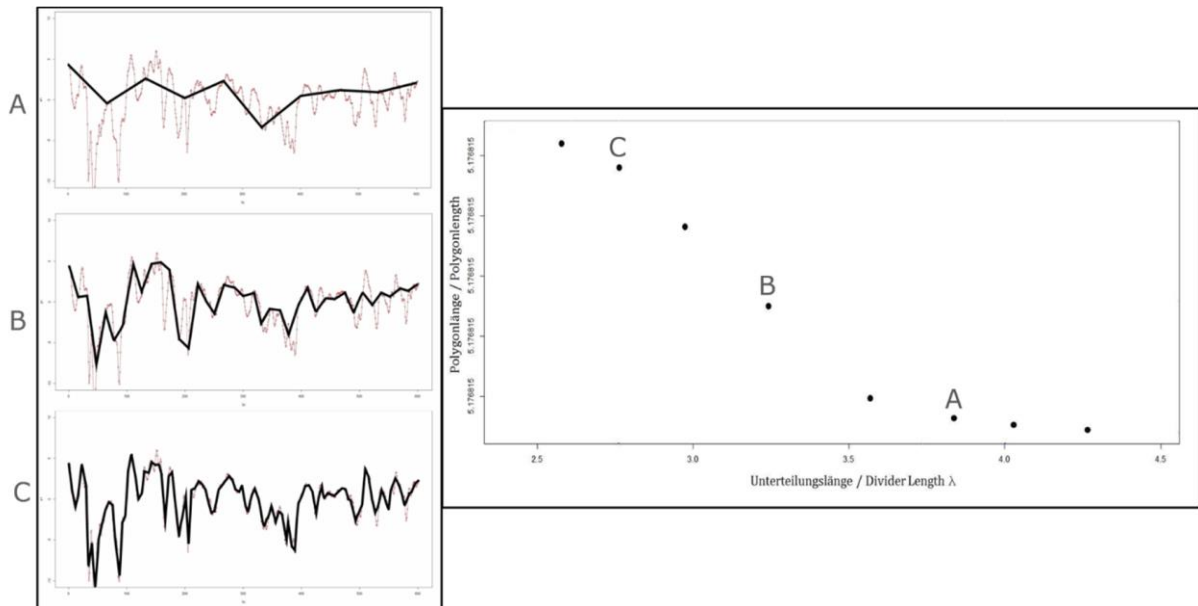
Figure 10: Iteration of sub-division length (left) and creation of Richardson plot (right) [17]

The segment lengths (abscissae) are plotted with the polygon lengths (ordinate) on a logarithmic scale. This so-called Richardson plot (Figure 10) delivers the fractal dimensions, described by regression lines. For railway track analyses, three dimensions are investigated, representing short-, medium- and long-wave track irregularities (Figure 11). The slopes of these three regression lines express the respective wave range in the data segment (=fractal values). Due to the negative slopes, fractal values are always below zero. [17]
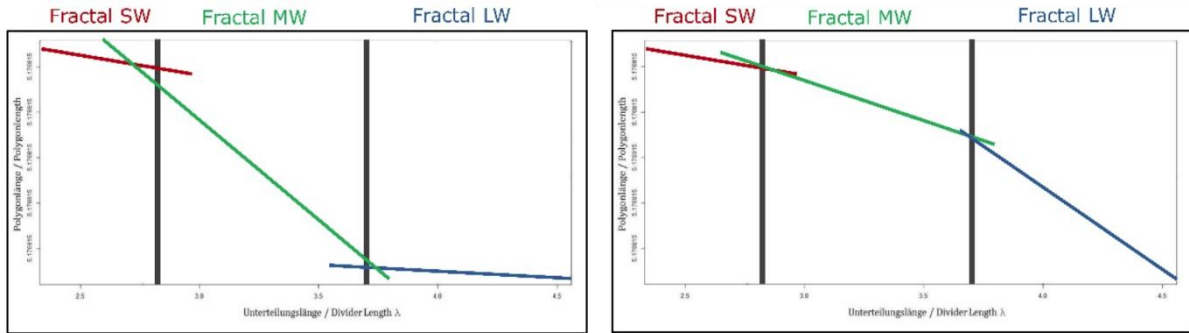
Figure 11: Richardson plot with increased gradient in the medium (left) and long wavelength range (right) [17]

Ballast bed condition is described by the medium-wave range. High fractal values indicate clean ballast, low values a contaminated bedding (left illustration in Figure 11). The long-wave range can be attributed to conditions in the lower ballast bed, the transition area, or even the substructure. The short-wave range is assumed to reflect problems with sleeper screws or disturbances in the contact area of sleeper and ballast. [17]

Figure 12 shows an exemplary result of a fractal analysis for the medium wavelength range which represents ballast condition. The graph highlights better and worse conditions, described by higher and lower fractal values. Additionally, past fractal analyses (bright lines) display the change of ballast condition over time.
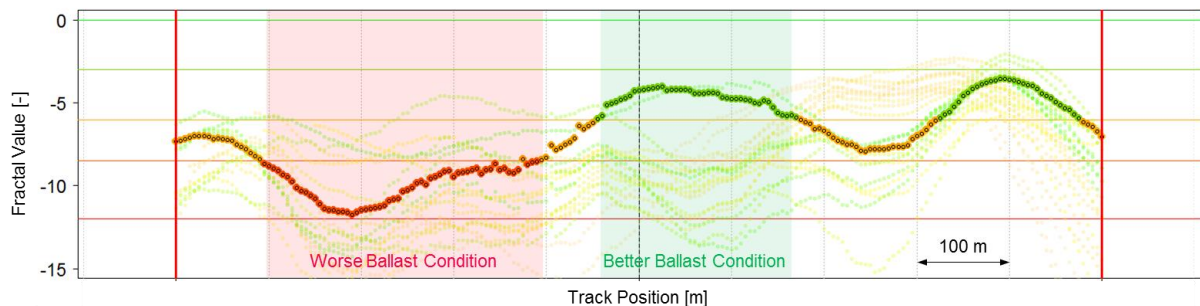
Figure 12: Example of fractal analysis for medium wavelength (ballast condition)

3 Tamping

The tremendous forces induced into track by train operation cause its deformation. When in adequate condition, tracks' elastic properties guarantee an almost complete return to the initial position after relief of the strain. However, this is not an everlasting state and permanent deformations, accelerated, amongst others, by inadequate ballast condition, are inescapable. Resulting irregularities of track geometry can be coped with in several ways:

- Slow orders prevent unsafe operation and mitigate dynamic forces, thus the track is protected. As these measures generally hamper train operation and create additional costs for railway undertakings, they should only be imposed temporarily in exceptional cases (rather than being the strategy of choice).
- The most frequent maintenance measure to tackle geometrical failures is levelling, lining and tamping (*maintenance tamping*).
- Ballast cleaning, which is automatically succeeded by a tamping action, sustainably enhances track alignment quality. However, this measure is expensive and only economically beneficial as maintenance action under specific circumstances [19].
- Track renewals, conducted with state-of-the-art machinery, create precise track geometry. In most cases, track renewals automatically include cleaning and/or exchange of the ballast bed. If necessary, substructure issues can be cured during this process too. These measures do not only correct track geometry, but also ensure a lasting amendment of overall track quality. After relaying a new track grid, tamping actions are mandatory to guarantee stability and durability of the system (*track renewal tamping*).

3.1 Tamping – Historical Overview

The importance of decent track alignment and stable sleeper bearing was already known long ago. While pickaxes had been the tool of choice before, electrical hand-held tamping units for ballast compaction were developed at the beginning of the 20th century. *Preussische Staatsbahnen* were the first to use them in 1916. [20]

Rising speeds and traffic density soon required more sophisticated tools. This growing demand was met by a tamping machine, introduced in 1938 by Swiss company *Scheuchzer SA* (Figure 13). Driven by a combustion engine and operated by one man, it was able to perform between 60 and 100 metres per hour. Vibrating tamping tines packed ballast under the sleeper until tamping forces succeeded a threshold value. This stopped the squeezing process and the operator moved the machine to the next sleeper. [21]
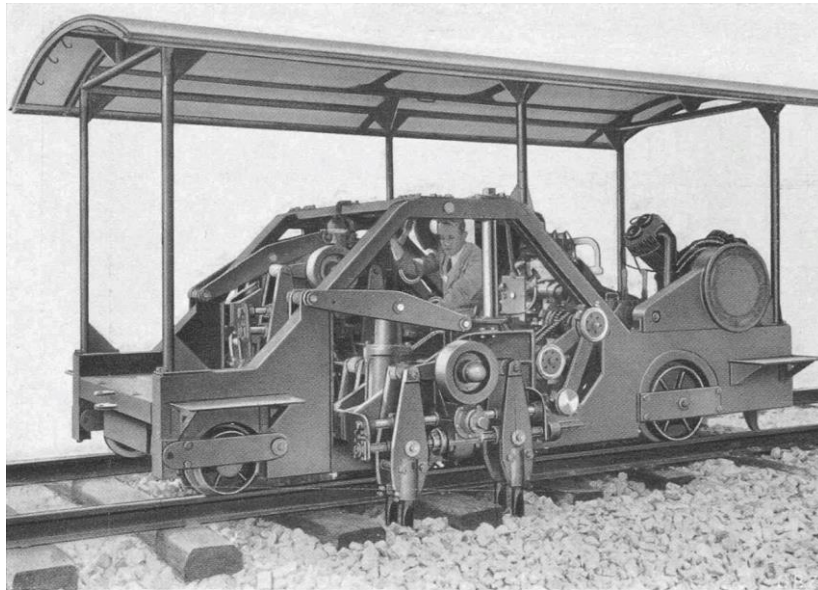
Figure 13: First self-driving tamping machine from 1938 [21]

The development of the first hydraulic tamping unit by Plasser & Theurer in 1953 was a big step towards sustainable track maintenance. Rather than moving equal distances, as tamping tines of mechanical systems used to, the hydraulics allowed all tines to travel different ways while applying equal pressures on the ballast. This guarantees uniform compaction of the rocks and creates homogeneous sleeper bearings. [22] Even though tamping machinery has been constantly improved over the last decades, it still relies on this principle. Some other important developments since the beginning of mechanised track alignment correction are: [23]

- 1962 turnout tamping machine
- 1965 2-sleeper tamping machine
- 1965 integration of track lining into the process (in addition to lifting)
- 1973 incorporation of dynamic track stabilisation
- 1983 separation of tamping machine and tamping satellite – first continuously working tamping machine
- 1996 3-sleeper tamping machine
- 2005 4-sleeper tamping machine

This ongoing development is no coincidence, but the answer to ever rising demands on railway infrastructure and equipment suppliers. Increasing traffic volumes, higher speeds and less time for maintenance must be compensated by technological progress of all players. Figure 14 makes this advance visible using the example of tamping machines.
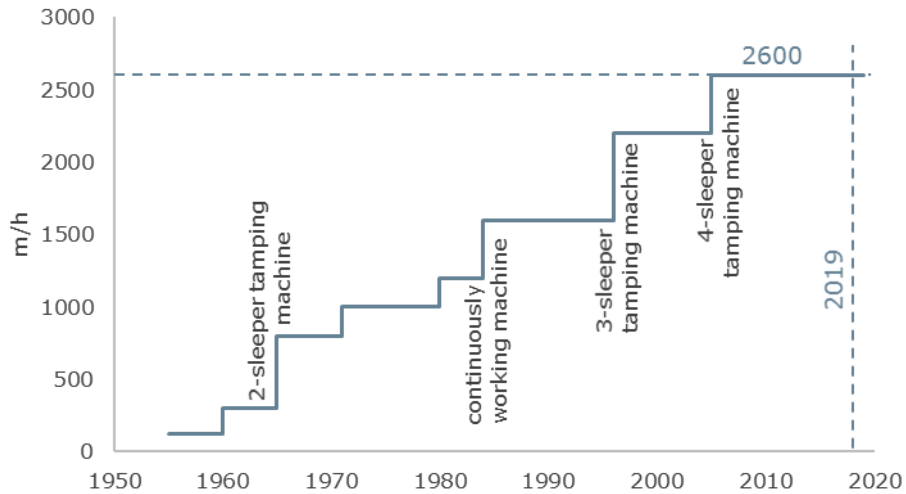
Figure 14: Development of "tamping output" per hour acc. to [24]

Not only has the working speed of tamping machines risen significantly since the early days, but the quality of the work has also improved substantially. Sustainable railway operation relies on durable track quality, which modern tools must deliver. [23] However, tamping performance in the sense of working speed is not always the main factor of concern. For example, when multiple single failures or turnouts need to be corrected, big mainline tamping machines lack the necessary flexibility. For suchlike requirements, specialized turnout or spot tamping machines have been developed. [25]

Measurement data used in this study were recorded by a 4-sleeper mainline tamping machine – *Dynamic Stopfexpress 09-4X E³* (Figure 15). Essential parts are marked in the image and explained in Chapter 3.2.

Figure 15: *Dynamic Stopfexpress 09-4X E³* [26]

3.2   Levelling, Lining and Tamping

Tamping actions consist of three main steps: lifting the track grid to the target height, laterally aligning it and consolidating the ballast under the sleepers in order to create a stable bearing.

3.2.1 Measuring System

A precondition for the correction of track alignment errors is the knowledge of current and desired track geometry. Only on this condition can the tamping machine bring rails and sleepers into the correct position. Figure 16 illustrates a simple tamping machine, which is used to explain how relative track geometry (balance of deviations of the existing track geometry) is established.
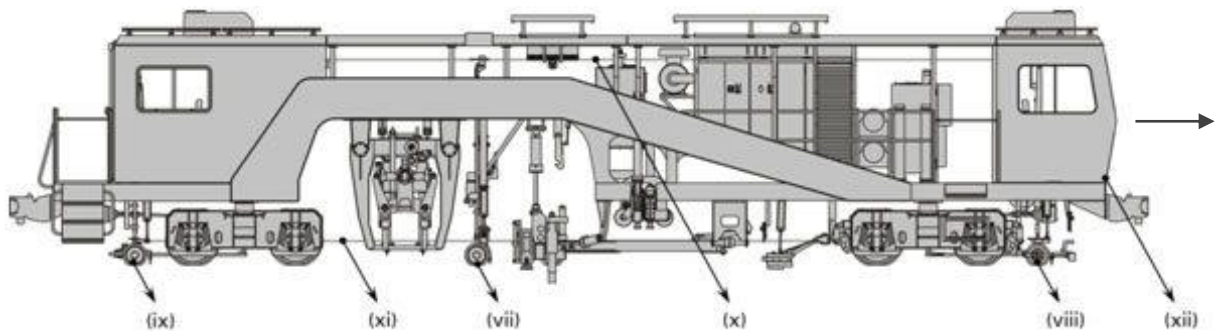
Figure 16: Simple tamping machinery [25]

The measuring system consists of three measuring trolleys, two serving as reference points at the front (viii in Figure 16) and rear (ix). The third one is positioned centrally (vii), next to the tamping unit. Two steel cords (x), one above each rail, extending from the rear to the front measuring trolley, provide a reference line for relative vertical track alignment. A third cord (xi), placed in the middle of the track, is used as reference for relative horizontal alignment. [25]
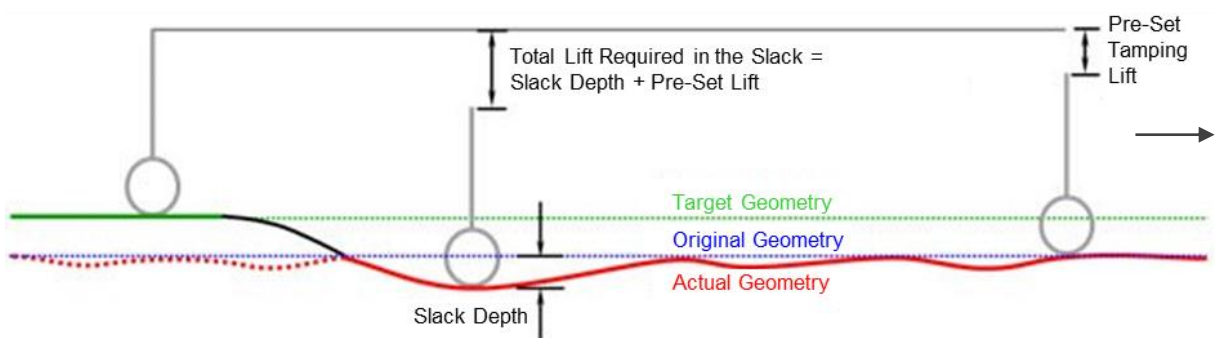
Figure 17: The lifting principle acc. to [25]

The total lift at each point is the sum of a pre-set tamping lift (at least minimum lifting height, see Chapter 3.3.1) and the current slack depth, illustrated in Figure 17. Horizontal adjustment is done equally but does not include a general pre-set displacement. This simple and robust system works well as long as the wavelength of the alignment error is shorter than the cord length. Otherwise, the entire tamping machine follows the defects without correcting them. This issue is counteracted by placing a mobile trolley about 100 to 150 metres in front of the tamping machine. A laser, or optical equipment, mounted on the mobile trolley, targets the front of the tamping machine. The machines' wires are then adjusted until the laser or the optical system aims centrally at a target board. This principle effectively lengthens the steel cords and enables correction of alignment issues which exceed machine length. [25]

With the above described system, track can be graduated, and relative unevenness eliminated. However, this system does not allow to move the track grid into a new position. This so-called *absolute geometry*, which is defined by fix points, requires pre-measurement of current track alignment via a geodesic survey or with a recording car as well as a defined target geometry. Based on these two input parameters, differences are calculated and passed to the tamping machine as correction values. [27]

3.2.2 Tamping Process

Prior to a tamping action, new ballast is added along the respective section. The tamping process itself begins with positioning the tamping unit and aligning the track, according to pre-determined vertical lift and lateral displacement (Chapter 3.2.1). Thereupon, one to three consecutive squeezing processes are performed. Each of them includes ballast penetration, squeezing movement and lifting the tamping unit (Figure 18).
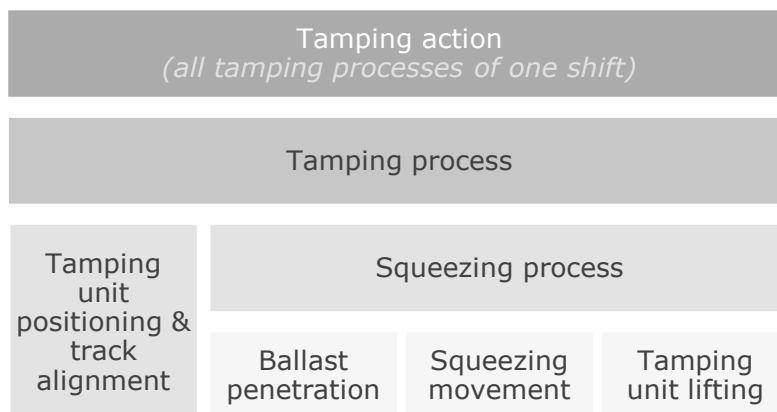
Figure 18: Elements of a tamping process

First, the tamping unit is positioned centrally above a sleeper (Figure 19, leftmost illustration). Most modern tamping machines, especially high-performance main line tamping machines, move continuously forward at a certain speed. The only component that comes to a halt for the tamping process is the tamping unit. Therefore, instead of stopping and accelerating the machine repeatedly, only the tamping unit itself is required to do so. This drastically reduces energy consumption and improves machine performance. [16]
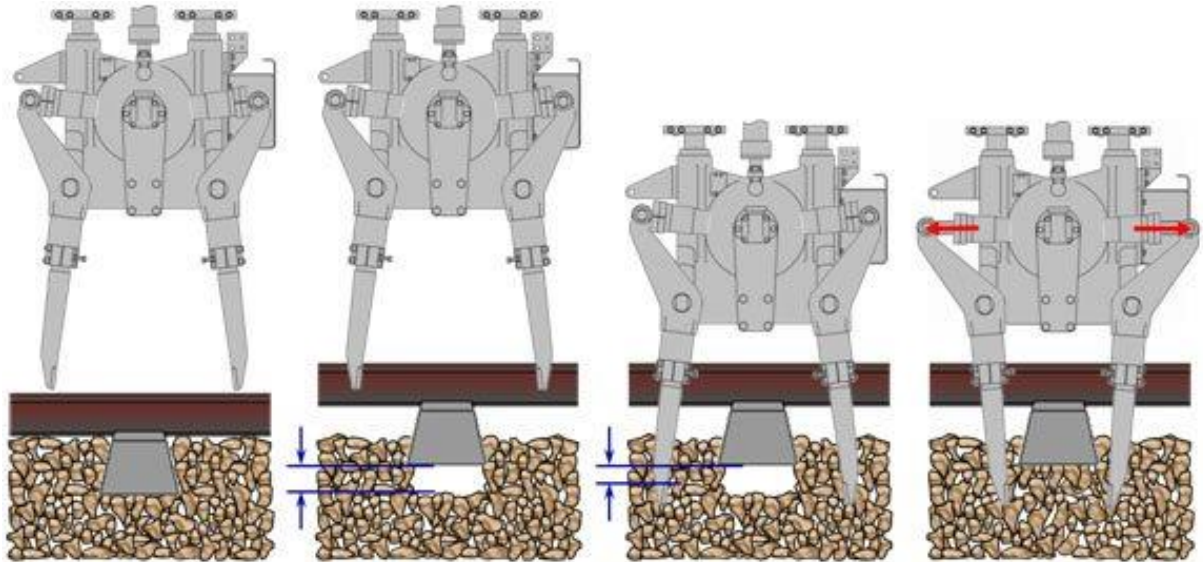
Figure 19: Tamping process description [25]

Once the tamping unit is in position, a lifting unit raises the track grid to the pre-determined height and simultaneously displaces it laterally, if necessary (Figure 19, second illustration). Next, the tamping unit is lowered and the constantly vibrating tamping tines (see Chapter 3.3.3) penetrate the ballast bed (Figure 19, third illustration). Immediately after reaching their final depths, the squeezing movement begins (Figure 19, rightmost illustration). Rising pressure in the hydraulics closes the tamping tines and thereby ballast underneath the sleeper gets compacted. Finally, the tines open and the tamping unit is lifted. Squeezing processes may be repeated once or twice on every sleeper, depending on ballast condition and required lift. [25]

3.3 Tamping Parameters

Success of tamping actions can be defined by quality and durability of the executed track. It depends on many factors, some of which are within the scope of the tamping machine. Such parameters must be considered when tamping units are calibrated. Below, the most important parameters are explained. If they are set improperly, the tamping action will fail to deliver desired results.

3.3.1 Lifting Height

Rearranging ballast underneath the sleepers requires vacant space in the ballast bed. This is automatically achieved when the track grid is lifted (Figure 19, second illustration). However, insufficient lifts (less than 15 or 20 millimetres, depending on grain size) impede relocation of the rocks. Subsequently, settlements can arise after the tamping action which may even exceed the lifting. Great lifts usually require a second or even third squeezing process to form a stable sleeper bearing. It should be mentioned that these are estimations for ballast with a main grain size of 20 millimetres; other grain size distributions may require different minimum lifting heights. [25]

3.3.2 Tamping Depth

A correct tamping depth, i.e. how far the tamping tines enter the ballast, is relevant for two reasons: If the tines penetrate the ballast too deeply, compaction underneath the sleeper remains uneven and incomplete. In contrast, too shallow insertion depth can damage sleepers during the squeezing process. Approximately 15-millimetre gaps between the bottom of the sleeper and the top of the tamping tine plate show optimal results (Figure 19, third illustration). [25]

3.3.3 Tamping Tine Oscillation

Tamping tines constantly vibrate during the tamping process. This oscillation is required to untighten the interlocked stones and enable rearrangement and consolidation. Additionally, it significantly reduces the required force to penetrate the ballast. Best compaction is reached at a frequency of 35 Hertz during the squeezing movement. Lower frequencies require higher forces and do not establish a dense matrix. Quicker oscillations liquefy the ballast and create plastic deformations (settlements). [1], [25]

The latest generation of tamping units incorporate frequency regulation. Higher frequencies during the penetration process facilitate entering the ballast bed. Lower frequencies during tamping unit relocation reduce wear of the gear. [22]
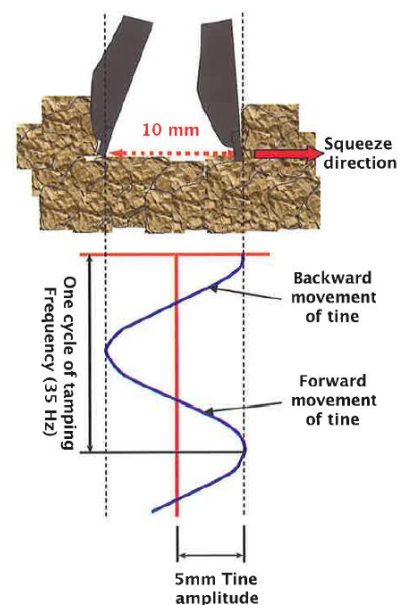
Figure 20: Tamping tine oscillation [25]

Besides frequency, the amplitude of the oscillation is an important factor too. Five millimetres forth and back movement (10 mm total travel, see Figure 20) are standard values. Lower amplitudes fail to transfer vibration energy into the ballast, while greater amplitudes tend to crush the rocks. [25]

3.3.4 Squeezing Velocity and Squeezing Time

The quality of tamping actions also depends on squeezing velocity and squeezing time. Premise is that the resistance of the interlocked stones is overcome. The required energy to loosen the matrix is transmitted during impulses between tamping tine and ballast stones. These impulses occur during the short period, when the forward oscillation superposes with the squeezing movement.

For efficient energy transfer from the tamping machine into the ballast, the impulse time should at least last 5 milliseconds. Considering this value and the above-mentioned oscillation frequency of 35 Hertz, a reasonable squeezing velocity of 150 millimetres per second can be calculated. Assuming that average squeezing distances are 120 millimetres, this velocity implies that squeezing time should be set to 0.8 seconds (up to 1.2 seconds, depending on ballast condition). [25]

3.3.5 Tamping Force

Even though the oscillation of the tines slackens the ballast structure, tamping units still generate very high forces to move and rearrange the rocks. Static tamping forces of 10 to 12 kN, measured at the tines, are required (Figure 21). [22]
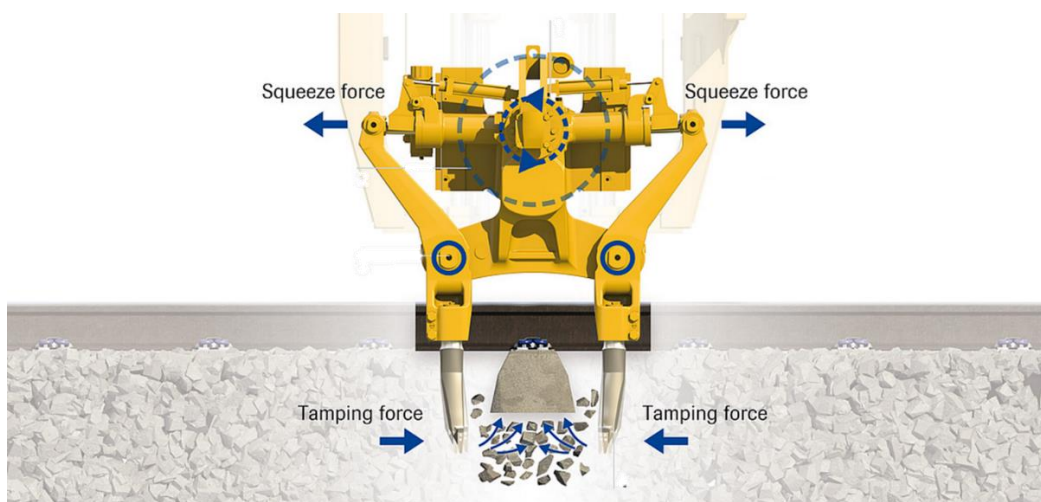
Figure 21: Tamping force [28]

In conclusion, all parameters explained on previous pages are listed in Table 2, together with commonly used values.

Parameter	Magnitude
Minimum lifting height	15-20 mm
Tamping depth	15 mm
Oscillation frequency	35 Hz
Oscillation amplitude	4-5 mm
Squeezing time	0.8-1-2 s
Squeezing velocity	150 mm/s
Squeezing distance	120 mm
Impact duration	5 ms
Tamping force	10-12 kN

Table 2: Important tamping parameters

3.4   Track Refurbishing Train

Oftentimes, tamping machines are not deployed solely but in combination with other machinery: a dynamic track stabiliser (DTS) and a ballast distribution system (BDS). While tamping creates consolidated bearings under the sleepers, other areas of the ballast bed are weakened during this process. When the tamping tines are lifted, loose spots remain between the sleepers. At the ends of sleepers, gaps between them and ballast can arise through lateral displacement.

A track stabiliser, following the tamping machine, initiates lateral oscillation of the entire track grid while contemporaneously applying vertical strain (see Figure 22). Through this vibration, rocks of the entire ballast bed rearrange and form a strong, homogeneous structure. Many modern tamping machines incorporate a dynamic track stabilisation system behind the tamping unit (see Figure 15). This scales the number of required vessels down to two. [29]
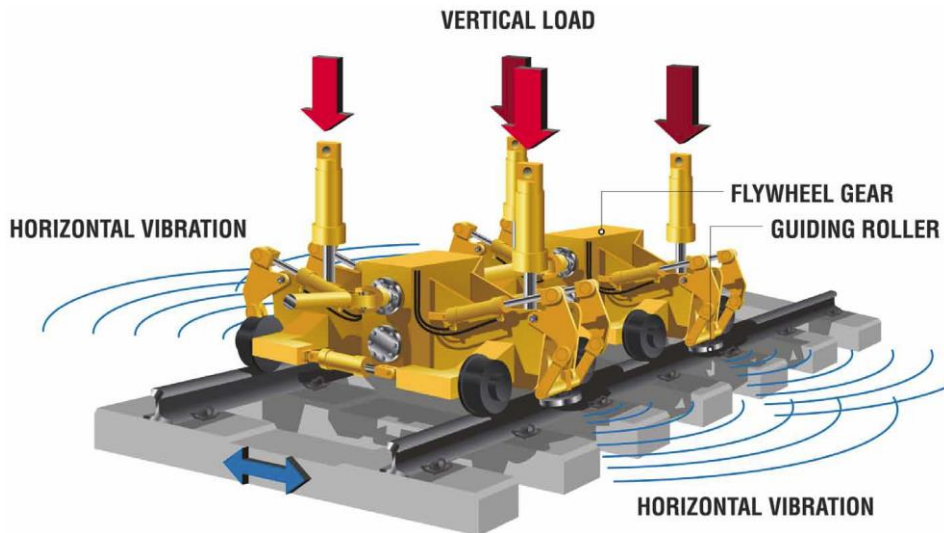
Figure 22: The principle of dynamic track stabilisation [29]

In Austria, a ballast distribution system (BDS) is deployed to complete the maintenance action by default. Compacting the ballast bed during tamping and subsequent stabilisation through the DTS reduces overall ballast volume. Therefore, additional ballast is unloaded on track prior to the tamping action. The BDS collects ballast in areas of abundance and deposits it where needed. At the same time, it profiles the bedding to create an even cross section. In combination, these machines (tamping machine, DTS, BDS) form a *track refurbishing train*. [30]

4 Data Sources

Evaluating possible correlations between ballast condition and tamping measurements requires two sources of information. One part is provided by the Institute of Railway Engineering and Transport Economy at Graz University of Technology. These data comprise all necessary information regarding infrastructure assets and track condition. They are later referred to as *Infrastructure Data*. The second input are recordings from a tamping machine, provided by Plasser & Theurer. These measurements are named *Tamping Data*.

Infrastructure Data
• Available information: asset data, track condition
• Provided by: Institute of Railway Engineering and Transport Economy / ÖBB Infrastruktur AG

Tamping Data
• Available information: recordings of different parameters during tamping actions
• Provided by: Plasser & Theurer

Figure 23: The two available data sources

4.1 Infrastructure Data

In cooperation with ÖBB-Infrastruktur AG, the Institute of Railway Engineering and Transport Economy preserves, updates and gradually expands an extensive data base of the Austrian railway network. Available information includes asset data, machine deployments, recordings of a monitoring car and analyses of measurement data. This sophisticated data warehouse is used for all kinds of research, studies and assessments, conducted by the Institute in cooperation with ÖBB-Infrastruktur AG.
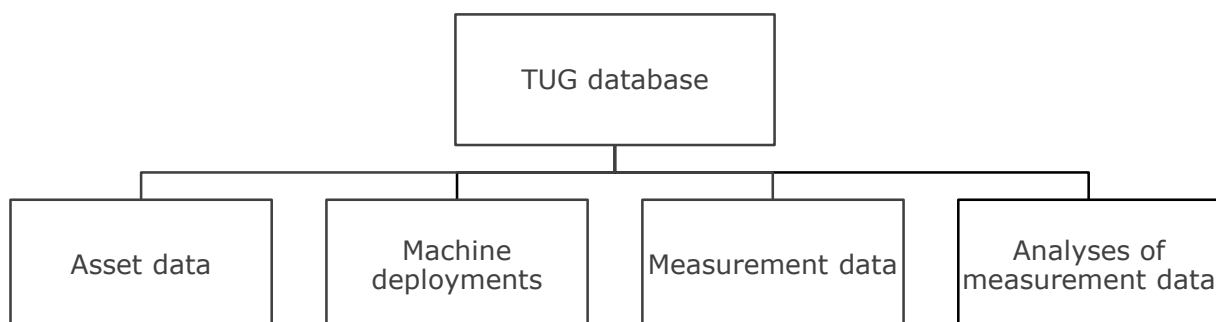
Figure 24: Available information TUG database

The database divides the core network into 23 lines. Furthermore, these lines are subdivided into the number of tracks on this line. Information is generally available in steps of five metres for every track. Any of these cross-sections is uniquely marked by the combination *line number–track number–track position (km)*.
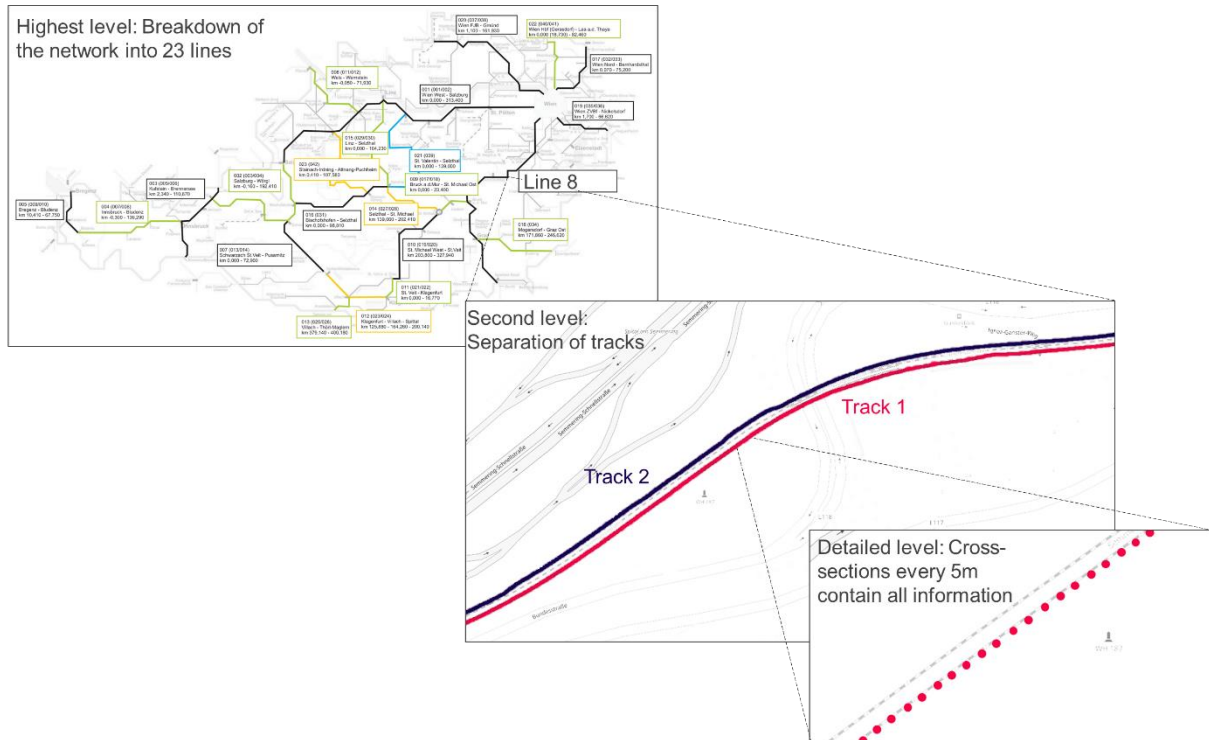
Figure 25: Structure of the TUG-database

Anent asset data, all specifications relevant for infrastructure managers and research institutes are available. These are:

- Number of tracks on the line
- Track load [tons per day]
- Curvature
- Rail profile
- Sleeper type
- Rail installation year
- Sleeper installation year
- Rail steel grade
- Line speed
- Installations (stations, bridges, turnouts, railway crossings, tunnels)

One information, which is important for this study but not explicitly listed in the data base, is ballast age. However, it can either be derived from sleeper age (installing new sleepers almost certainly includes ballast exchange) or deployment of ballast bed cleaning machines. Whichever happened last, is assumed to be the installation year of the ballast bed.

Next to asset data, recordings of past maintenance measures are essential to understand the effects of track works. Measures executed with mechanized track machinery have been recorded since 1999. Date and location of the following machine deployments are known:

- Track refurbishing train (tamping machine + DTS + BTS)
- Formation rehabilitation machines
- Track renewal trains
- Ballast bed cleaning machines
- Rail grinding machines

Particularly important for infrastructure managers is the knowledge of current track condition. At the Institute of Railway Engineering and Transport Economy, all measurements of ÖBBs monitoring car since 2001 are available for research purposes. The entire network is recorded three to four times a year. Measured parameters include:

- Vertical alignment
- Horizontal alignment
- Gauge
- Superelevation
- Cant

In addition, data recorded by ground penetrating radar are available too. However, this is still a relatively new technology and not the entire network has been inspected yet.

Raw measurement data are only one part of track condition assessment. More precise information is gained by applying various algorithms. These deepening analyses enable evaluations of parameters which are not explicitly recorded as well as condition assessment of single components. Gained knowledge fosters the understanding of tracks and helps improve the Austrian and other countries' networks. One example is the fractal algorithm, which utilizes track alignment to assess lower levels of the track.

4.2 Tamping Data

Plasser & Theurer Export von Bahnbaumaschinen Gesellschaft m. b. H. have equipped tamping tines of one tamping machine with multiple sensors. *Dynamic Tamping Express 09-4X E³*, the machine in question, operates in the Austrian network and records different parameters during every tamping process.

The sensors were mounted on four of the machine's 64 tamping tines (see Figure 26), number 59, 60, 63 and 64. Data used in this study were recorded by tamping unit 3, tine number 64.
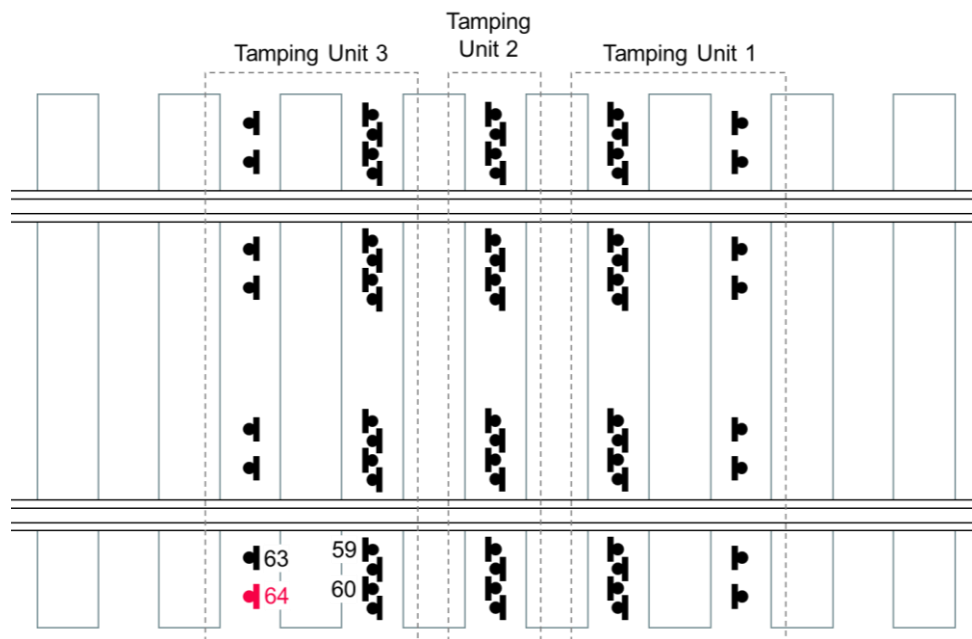
Figure 26: Tamping tines array acc. to Plasser & Theurer

To obtain as much information as possible on ballast condition, four different types of sensors were installed (arrangement see Figure 27): [31]

- Strain gauges: lowering and lateral forces
- Accelerometers: accelerations axial and tangential to the tamping arm
- Laser distance measurements: squeezing displacement (length of hydraulic cylinders whilst opening and closing)
- Pressure measurement: pressures in the hydraulic cylinders
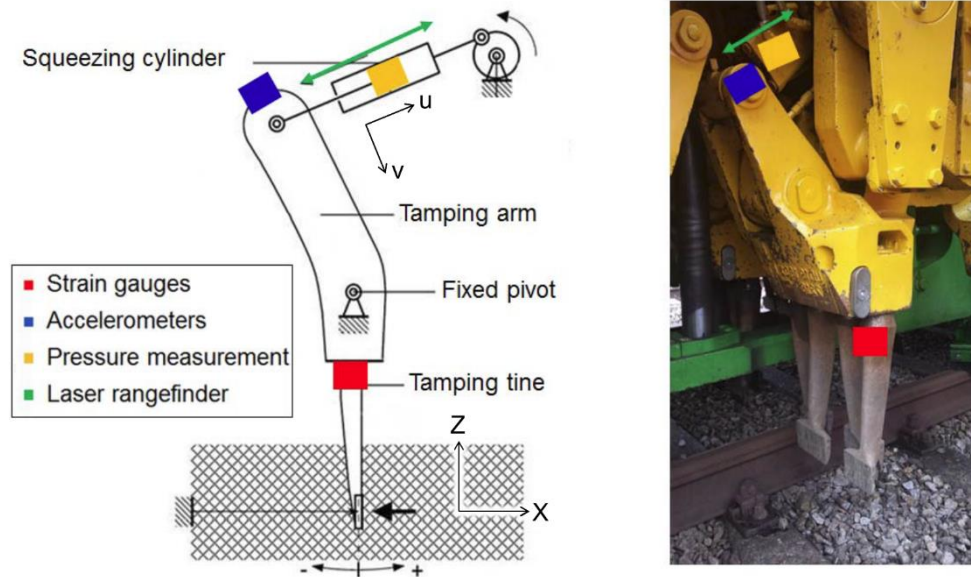
Figure 27: Positioning of the sensors [31]

The Institute of Geotechnics at TU Wien conducted a study on measurements of the tamping machine, focusing on material behaviour during the tamping process. In the study, researchers plotted load (ordinate) and displacement (abscissa) in a diagram. This common way of displaying dynamic measurements enables exploration of material behaviour under strain. The study found a typical pattern during the squeezing movement, presented in Figure 28. The illustrated "butterfly-diagram" represents one cycle (one oscillation of the tamping tine) while the tines are closing. [31]
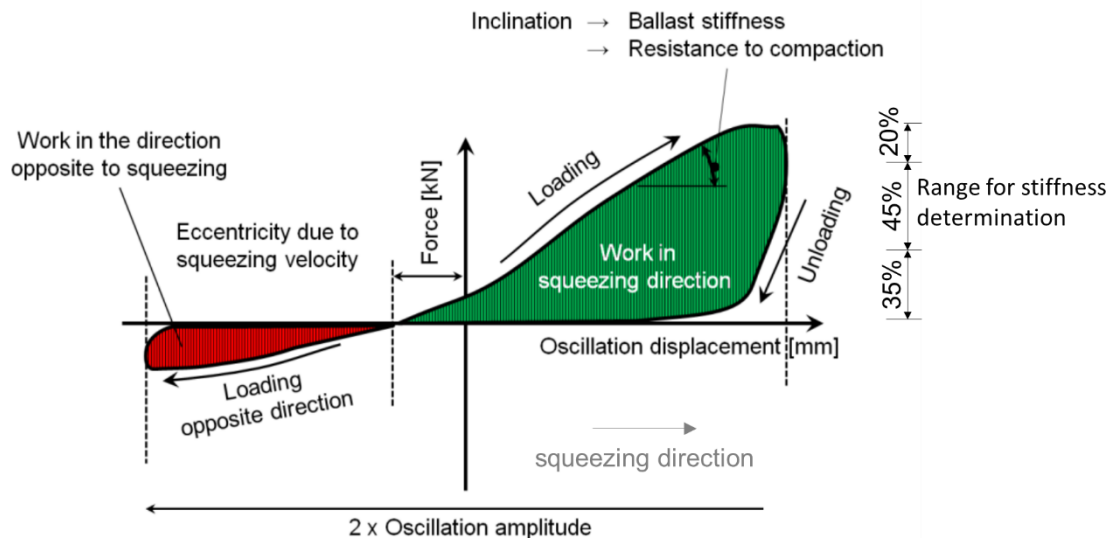
Figure 28: Typical load-displacement curve [31]

The later analysed parameters *energy* and *stiffness* become visible in the load-displacement diagram. When tine oscillation and squeezing movement shift in the same direction, the lateral force steadily increases, up to the point where the tine reaches its maximum amplitude and moves back towards its dead position. The angle the curve encloses with a
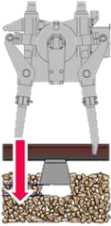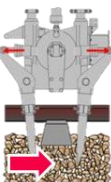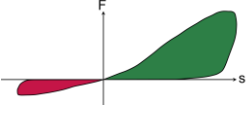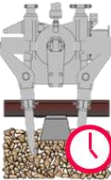
horizontal (middle 45% are considered), represents ballast's resistance to compaction, i.e. its stiffness (later referred to as *Loading Stiffness*). Having turned around, the tine moves opposite to the squeezing direction, which leads to an abrupt drop in lateral force. The angle between this part of the curve and a horizontal is named *Unloading Stiffness*. Depending on ballast condition, this parameter can take positive or negative values. The difference between *Loading* and *Unloading Stiffness* describes the plastic deformation of the ballast. [31]

Important for the success of a tamping process is the transfer of energy from the tamping tines into the ballast bed. This energy is represented by the area enclosed by the load displacement curve (see Figure 28).

In addition to these parameters (*Energy per Squeezing Movement*, *Loading Stiffness*, *Unloading Stiffness*), four others are provided: *Penetration Force*, *Squeezing Force*, *Squeezing Time* and *Squeezing Velocity*. All available parameters are listed and described in Table 3.

Penetration Force [kN]		maximum axial force (in z-direction) during ballast penetration
Squeezing Force [kN]		maximum lateral force (in x-direction) during squeezing movement
Energy per Squeezing Movement (*Squeezing Energy*) [J/s]		standardized consumed energy per squeezing movement (average of all cycles)
Squeezing Time [s]		duration of the squeezing movement (as this is a pre-set value, it is not used for ballast condition evaluation)
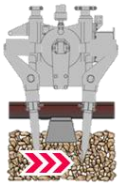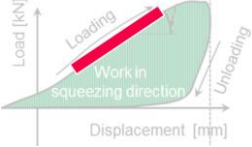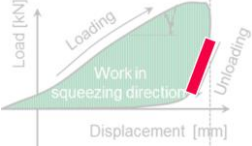
Squeezing Velocity [mm/s]		velocity of the closing tamping tines
Loading Stiffness [MN/m]		stiffness during forward oscillation of the tamping tine (average of all cycles)
Unloading Stiffness [MN/m]		stiffness during backward oscillation (average of all cycles)

Table 3: Analysed measurement parameters

5 Data Preparation and Connection

Working with data of any kind usually requires their preparation prior to evaluations. Frequently necessary steps are reasonably formatting the data, filtering relevant information, treating outliers or measurement errors, calculating missing values or parameters and more. As the data analysed in this study originate from two sources, different measures were required to make them feasible.

5.1 Preparation of Infrastructure Data

Most information of the Austrian railway network is available every fifth metre of track. While this level of detail is generally sufficient, the current research benefits from more detailed information, at best in steps of one metre. Of all available information, sleeper types, maintenance actions and ballast condition (from ground penetrating radar and fractal analyses) are relevant.

5.1.1 Asset Data and Machine Actions

Besides installations like turnouts or short bridges (which are removed later and therefore do not matter), asset data are generally constant over long sections. In order to get information for every single metre, the database is expanded by duplicating the original entries. Every cross-section is multiplied four times – the two previous and the two following points are assigned the original data. This step does not provide additional information but simplifies the connection of infrastructure and tamping data. Figure 29 exemplarily demonstrates how this process enlarges the database.

Original Data Set

Line	Track	Kilometre	Unique TUG-Key	Asset_Data	Machine_Action
…	…	…	…	…	…
8	1	40055	8_1_40055	a	1
8	1	40060	8_1_40060	a	2
8	1	40065	8_1_40065	b	3
…	…	…	…	…	…

Expanded File

Line	Track	Kilometre	Unique TUG-Key	Asset_Data	Machine_Action
…	…	…	…	…	…
8	1	40053	8_1_40053	a	1
8	1	40054	8_1_40054	a	1
8	1	40055	8_1_40055	a	1
8	1	40056	8_1_40056	a	1
8	1	40057	8_1_40057	a	1
8	1	40058	8_1_40058	a	2
8	1	40059	8_1_40059	a	2
8	1	40060	8_1_40060	a	2
8	1	40061	8_1_40061	a	2
8	1	40062	8_1_40062	a	2
8	1	40063	8_1_40063	b	3
8	1	40064	8_1_40064	b	3
8	1	40065	8_1_40065	b	3
8	1	40066	8_1_40066	b	3
8	1	40067	8_1_40067	b	3
…	…	…	…	…	…

Figure 29: Duplicating asset and machine action data

Due to the level of detail of the original data set, small errors cannot be avoided. For example, it is unknown at which exact point in the five-metre interval a parameter changes or where precisely a maintenance action began and ended. However, compared to analysed section lengths of hundreds of metres, this error is insignificantly small.

5.1.2 Ground Penetrating Radar

Ballast and substructure condition evaluated by the ground penetrating radar is available at every single metre appropriately formatted. Hence, no sort of data preparation was necessary.

5.1.3 Fractal Analyses

As fractal analyses are computationally extensive, the resolution of the algorithm is set by default to five metres. In contrast to discrete asset data, continuous fractal values cannot simply be duplicated without generating a significant error. Thus, fractal analyses are re-calculated for this study, delivering values for every metre.

Usually, when assessing track condition via fractal analyses, multiple fractal curves, calculated with the latest monitoring car recordings, are plotted concurrently. Not only does that

show behaviour over time, it also prevents judging the condition based on a single measurement, which might be biased.

Correlations of all tamping machine parameters with every computed fractal analysis are not constructive – 364 results would have to be examined (four recording car runs per year over 13 years allow 52 fractal analyses; each of them can be correlated with all 7 recorded tamping parameters). On the other hand, a single fractal curve lacks expressiveness, as described above. Therefore, an average or quartile value of several fractal curves is reasonable. All fractal analyses between fall 2013 (GPR recordings date back to this time) and spring 2017 (the maintenance actions were executed during this period) are included.

To assess which average value best describes all fractal curves, two test sections with a length of three kilometres each, one of which is plotted in Figure 30, are examined. The illustration shows 25%-quantile[3], mean, median and 75%-quantile of the considered fractal analyses. Although they all show similar characteristics, the strength of their peculiarities varies. The 25%-quantile is chosen for further analyses as it shows the highest fluctuations, hence it will produce most distinct results.
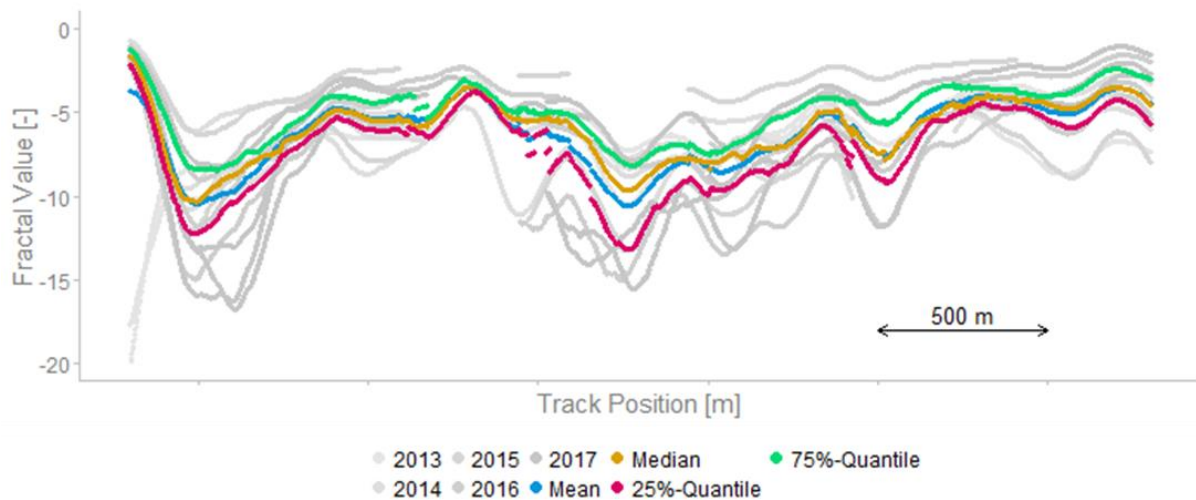
Figure 30: Average fractal curves

In addition, the curve is smoothed by calculating a gliding mean over 100 metres. This removes saltus, which can occur at start and end points of individual measurement car runs (see Figure 31).

---

[3] Quantile: divides a dataset into two parts – x% of the data are lower than the quantile value
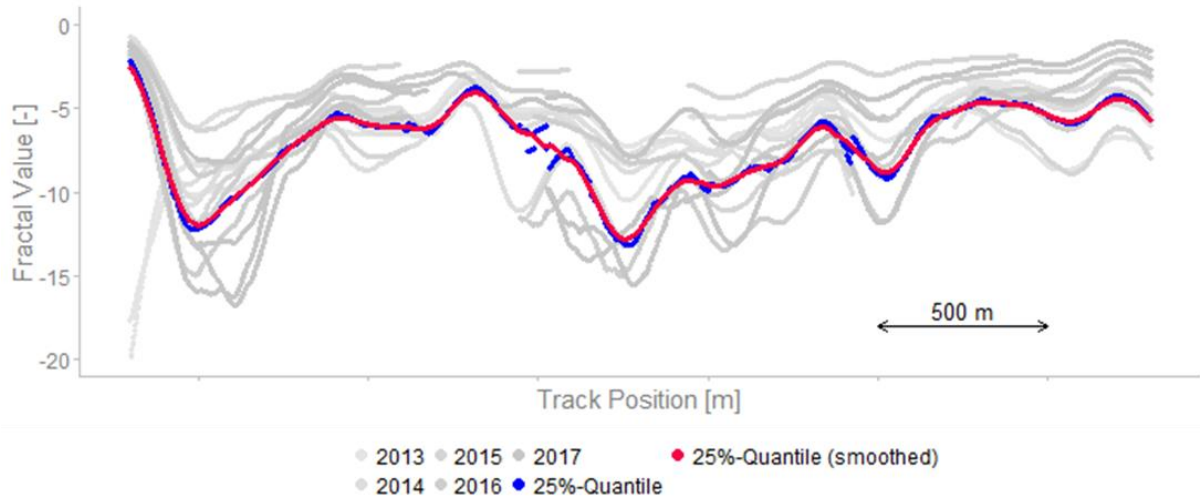
Figure 31: Smoothed 25%-quantile fractal curve

5.2 Preparation of Tamping Data

Data recorded by the tamping machine plus subsequently calculated parameters (energy, stiffness, velocity) were transmitted in form of 13 excel files, one for each tamping action. All files are equally structured: The file names specify date and location of the tamping actions. Ascending numbers mark every tamping process, geographical coordinates (latitude, longitude, height above sea level) specify the exact position of the tamping unit during the process. Additionally, the precise time of day is recorded. Besides this general information, the seven tamping parameters (see Chapter 4.2) are listed. In case of two squeezing processes at the same spot, two values per parameter are provided. When all 13 files are combined, a total of 9620 recorded tamping processes are available. However, this includes some erroneous recordings displaying only zeros rather than actual measurements. They are removed before further evaluations are conducted.

Tamping processes which required two consecutive squeezing processes are analysed for correlations between the squeezing processes. If recordings of the first squeezing process significantly correlate with values of the second process, they are expected to behave similarly. Thus, when comparing tamping data to infrastructure data, it does not matter if measurements of the first or second squeezing process are considered. Resulting trends will be similar. Therefore, only data of the first squeezing process are analysed for multiple reasons:

- The total number of possible correlations is reduced and excessive complexity avoided.
- Measurements of a second squeezing process are already influenced by the first squeezing process – they are not dependent solely on ballast condition anymore.

- Not all tamping processes required two squeezing processes – fewer available data limit achievable precision.

The strength of dependency between two metric variables is expressed by the Pearson correlation coefficient (Figure 32). In this study, it describes whether measurements of the first and second squeezing process are related (e.g. if the *Penetration Force* is very high during the first squeezing process, is it also very high during the second squeezing process?). The correlation coefficient can attain magnitudes between -1 and 1, the first representing a perfect negative correlation and the latter a perfect positive correlation.
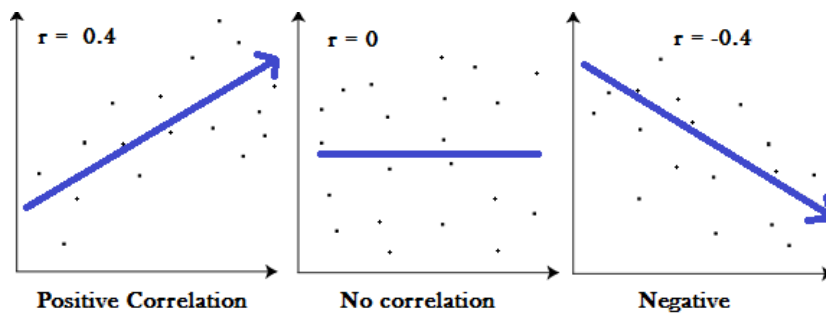
Figure 32: Pearson correlation coefficient [32]

The coefficient describes a linear dependency of two variables x and y, but it does not identify whether the correlation is significant. For clarification, a significance test is performed: Hereby it is tested if a null hypothesis, stating that there is no correlation between x and y, can be rejected or not. The correlation is called significant, if a calculated probability value p is below a chosen significance level. If so, the null hypothesis is rejected and an alternative hypothesis, stating that there is in fact a correlation between x and y, becomes true. Generally, the significance level is set at 5% (0.05). Table 4 illustrates the determined correlation coefficients and their respective probability values for all tamping parameter pairs.

First Squeezing Process	Correlation Coefficient	p-Value	Second Squeezing Process
Penetration Force 1	0.415	2.20E-16	Penetration Force 2
Squeezing Force 1	0.702	2.20E-16	Squeezing Force 2
Energy per SM 1	0.726	2.20E-16	Energy per SM 2
Squeezing Velocity 1	0.882	2.20E-16	Squeezing Velocity 2
Squeezing Time 1	0.509	2.20E-16	Squeezing Time 2
Loading Stiffness 1	0.584	2.20E-16	Loading Stiffness 2
Unloading Stiffness 1	0.117	3.10E-06	Unloading Stiffness 2

Table 4: Correlation coefficients and probability values

As all probability values are below 0.05, all parameters significantly correlate between the first and second squeezing process. When evaluating ballast condition in Chapter 7, only measurements obtained during the first process are considered.

5.3 Connecting the Data Sets

Premise for a comparison of data from two different sources is a link between them. In this case, only the geographical position can be used as a connector of infrastructure and tamping data. However, infrastructure data are assigned a position via *line-track-kilometre* while tamping data are located via *latitude-longitude-height*. Fortunately, data recorded by the ground penetrating radar include both track positions and corresponding coordinates. Hence, geographical coordinates are available in both data sets and GPR data are used as merging tool.

As explained in Chapter 2.4.1, not the entire network of ÖBB Infrastruktur AG has been inspected by ground penetrating radar yet. This means, not all of the 13 recorded tamping actions can be linked to infrastructure data. However, most tamping data originate from works on *Südbahn* (Vienna to Tarvis / Vienna to Spielfeld-Straß), which is one of the already GPR-evaluated lines. Therefore, the majority of provided data can be used.

Before connecting the two data sets, it must be assured that tamping data are linked to the correct track. Coordinates recorded by the tamping machine at every tamping process are not precise enough to specify which track was tamped. However, date and location of the tamping actions are known and can be compared to recordings of machine deployments which are available in the TUG database. Hence, the exact track can be determined and a correct connection of tamping data and infrastructure data, which is done by a VBA (Visual Basic for Applications) algorithm, is guaranteed.

Even though infrastructure data and tamping data include geographical coordinates, these coordinates are not equal. First, they are supplied with different accuracies (decimal places), which is problematic for an algorithm looking for a precise number. Furthermore, they are delivered at different track positions – in case of GPR data at every metre, in case of tamping data at every fourth sleeper. Additionally, the coordinates may have a general offset, particularly in areas where it is difficult to receive GPS signals (e.g. Semmering). For best possible results, data measured by the tamping machine are linked to the nearest point on the railway line (always considering the correct track). The shortest distance between two geographical coordinates can be calculated with the *haversine* formula [33]:

$$d = R * haversin-1(haversin(\phi2 - \phi1) + cos\phi1cos\phi2haversin(\lambda2 - \lambda1)).$$

$$haversin(x) = \sin^2\left(\frac{x}{2}\right)$$

Formula 1: Haversine formula [33]

d … distance between the points

R … earth radius (6371 km)

Φ_1, Φ_2 … latitude 1, latitude 2

λ_1, λ_2 … longitude 1, longitude 2

The connection algorithm works as follows: The first coordinate of the tamping data is taken and the distances to every coordinate of the infrastructure data are calculated, considering the correct track. Next, it searches the smallest calculated value, hence the shortest distance. This pair of coordinates is then stored together with its unique tamping process number and its unique TUG key. With these two keys, the two data sets can be linked. This procedure is repeated for every tamping process.

Figure 33 shows an exemplary section on the southern line (around Spital am Semmering) illustrating the connection algorithm. Both yellow lines show coordinates of the two tracks as recorded by the ground penetrating radar. Due to their accuracy, they are assumed to have been re-treated. The darker of the two yellow lines marks track 1, where the tamping action was executed. Light blue points represent coordinates recorded by the tamping machine, one for every tamping process (equals one or two squeezing processes). Partially, they show huge lateral offsets of up to 49 metres. On average, the shortest distance, thus the gap between tamping coordinates and infrastructure coordinates, is 8.2 m.
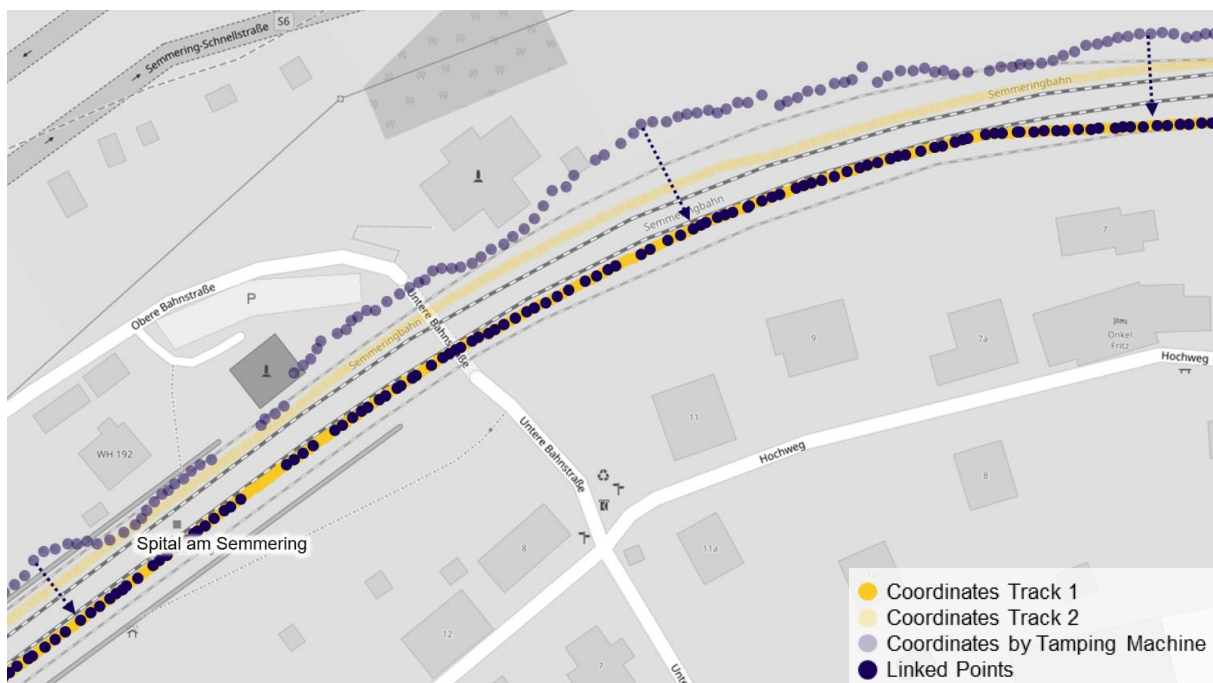
Figure 33: Exemplary illustration of the connection algorithm

For every light blue point, the nearest dark yellow point is determined and turned dark blue. Thus, tamping processes are projected onto the track. As lateral offsets are eliminated, it is most likely that the tamping process occurred in that place. Hence, the data sets are connected and dark blue points highlight cross sections on the track which contain all required information on infrastructure data and tamping data.

5.4   Treatment of Extreme Values

In data science, single measurements, which significantly defer from others, are usually marked as outliers and excluded from evaluations. Supposedly, they do not represent real conditions but vary due to other influences, e.g. measurement issues. As for infrastructure data, this step is not necessary: nominal asset data and ordinal GPR results cannot exhibit extrema. Fractal data could feature such extreme values. However, in this case they are calculated as gliding mean of the first quartile – thus, they have been averaged twice (see Chapter 5.1.3) and outliers at single points are impossible.

Tamping data include some measurements which strongly deviate from surrounding values. They are assumed not to accurately reflect ballast condition. A machine learning algorithm is applied in order to detect and subsequently remove these "non-fitting" recordings. The DBSCAN (density-based spatial clustering of application with noise) calculates distances between all points in a multi-dimensional space. Based on those distances, the points are clustered and, if not fitting in any cluster, marked as noise. [34]

All tamping parameters are treated separately, each time forming a 2-dimensional space between them and track position. Since the algorithm calculates Euclidian distances between points, the scales of the axes should be comparable. In this case, however, the x-axis represents track position in metres, and the y-axis machine measurements in their respective units. Using *Loading Stiffness* as example, the x-axis would take values from 40.000 to 115.000 (track kilometre 40 to 115) and the y-axis values from zero to eight. Thus, Euclidian distances in x-direction outstrip y-direction by several decimal places. The algorithm would not deliver reasonable results. By normalizing the parameters prior to algorithm application, this issue is dodged. Both x- and y-axis are brought into range of zero to one whilst keeping the points' relative position. After the algorithm has finished, the data are denormalized, hence their original magnitudes are restored. Figure 34 presents the result of the DBSAN algorithm using the example of *Penetration Force*: grey points are kept and red points removed.
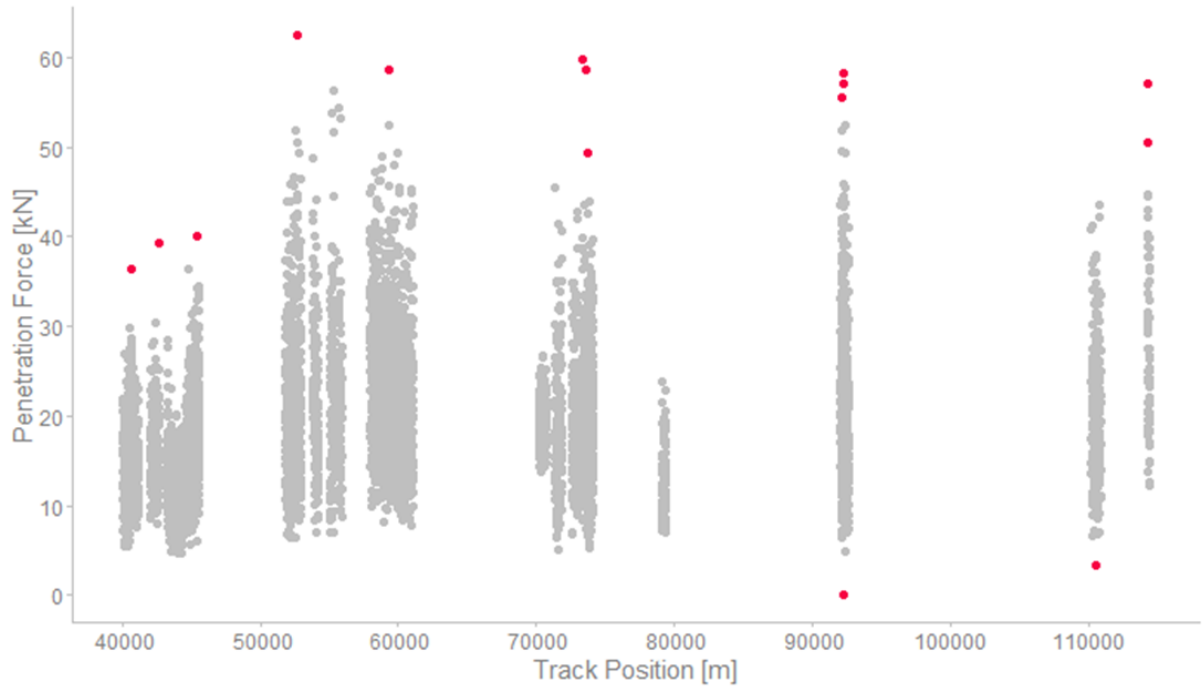
Figure 34: Outlier removal of *Penetration Force*

6 Data Analysis and General Results

In this chapter, all utilized data are analysed and some general results are presented. First, the GPS data of the tamping machine are made visible and conclusions, drawn from these data, are explained. Next, two recorded tamping parameters are compared to generally accepted values as stated in literature. The following part is devoted to evaluations of assets and ballast condition on the executed sections. Finally, tamping data are examined in more detail.

6.1 Evaluation of GPS Data

All available tamping data were recorded during 13 tamping actions, executed between July 2016 and April 2017. Apart from short sections in Styria, all of them were performed in Lower Austria, most on *Südbahn* between Sollenau and Mürzzuschlag.
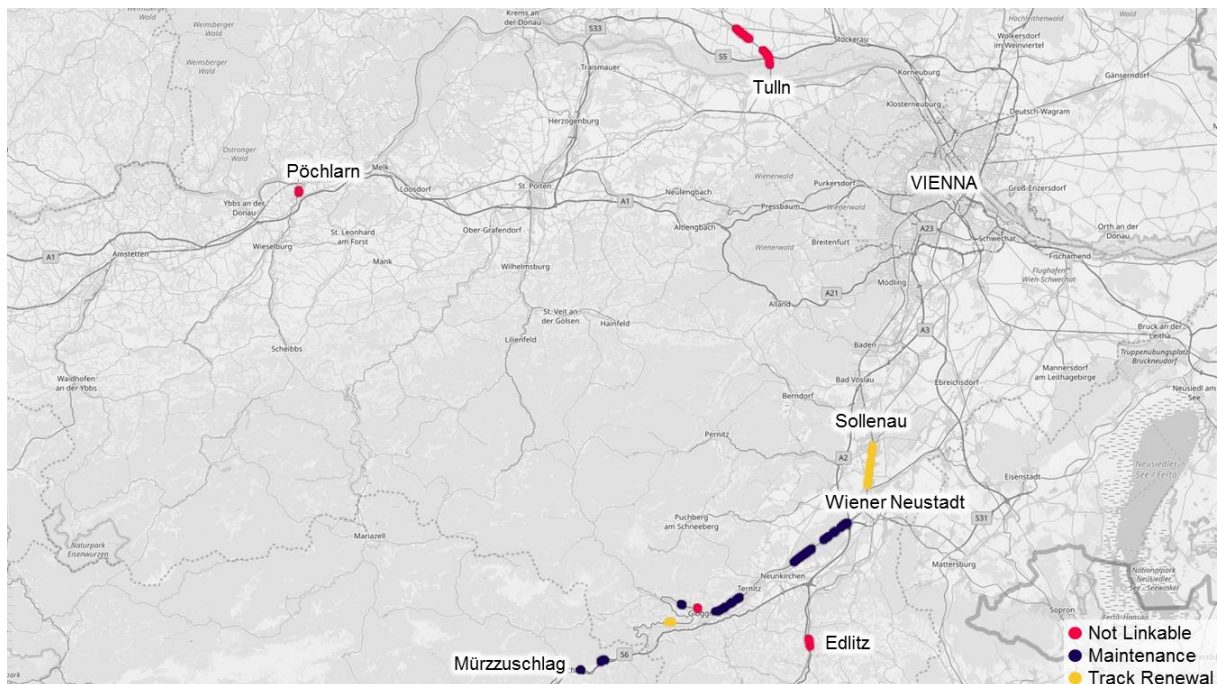
Figure 35: Overview of tamping actions

As explained in the previous chapter, connecting infrastructure data and tamping data is only possible if both feature GPS data. For this reason, tamping actions in Pöchlarn, Tulln and Edlitz cannot be linked, due to lacking information on the part of infrastructure. The same is true for a short section on the southern line. Although GPS data are generally available for this part of the network, there is a small data gap near Semmering (red points in Figure 35). In total, 2772 of the 9620 tamping processes are unable to connect to infrastructure data. The remaining 6848 data points are composed of 3712 maintenance and

3136 track renewal tamping (executed within the first couple of days after the track has been renewed) processes.

All recorded track work on the southern line was done between track kilometre 40 and 115, i.e. between Felixdorf and Mürzzuschlag. To a high degree, track 1 was maintained or renewed (Figure 36).
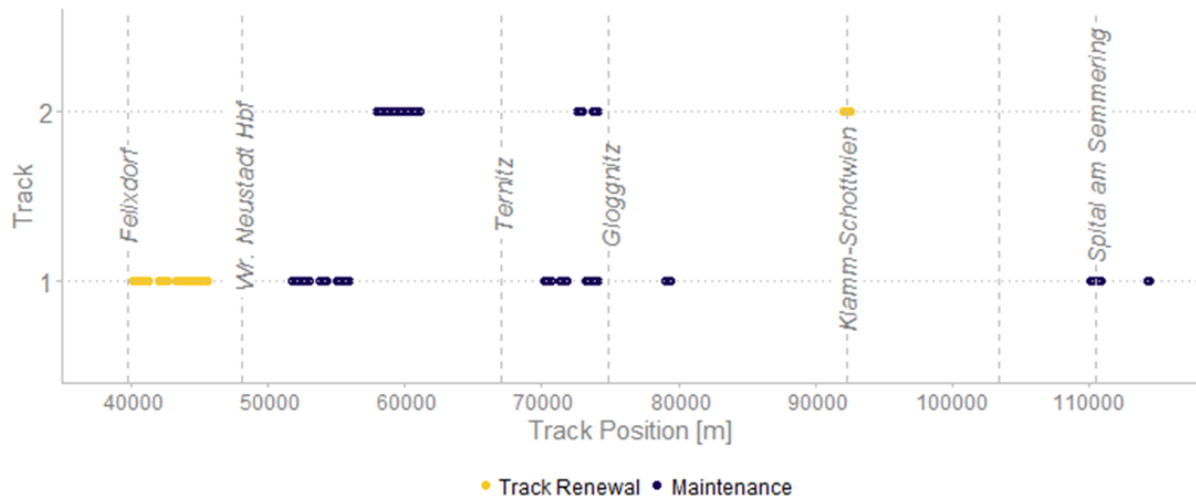
Figure 36: Tamping actions on *Südbahn*

By applying the haversine formula (see Chapter 5.3), distances between individual tamping processes can be calculated. On average, this gap is 2.43 metres. Considering that the tamping machine handles four sleepers at once and that the gap between two sleepers should be 60 centimetres per default, this value is reasonable. The average duration between two tamping processes, i.e. one or two squeezing processes plus repositioning the tamping unit, is 5.71 seconds. On the basis of these two values, an average machine performance of approximately 1500 metres per hour can be calculated.

6.2   Comparison of Literature and Tamping Data

Two of the parameters explained in Chapter 3.3, squeezing time and squeezing velocity, are recorded by the sensors on the tamping tines. This enables a comparison of generally accepted values and machine measurements.

6.2.1 Squeezing Time

According to literature, the optimal squeezing time lies between 0.8 and 1.2 seconds, depending on ballast condition [25]. This parameter can be set by the machine operator. Therefore, it is a subjective value depending on labour experience. Figure 37 shows a histogram of recorded squeezing times and the range where these values are expected to be (between 0.8 and 1.2s).
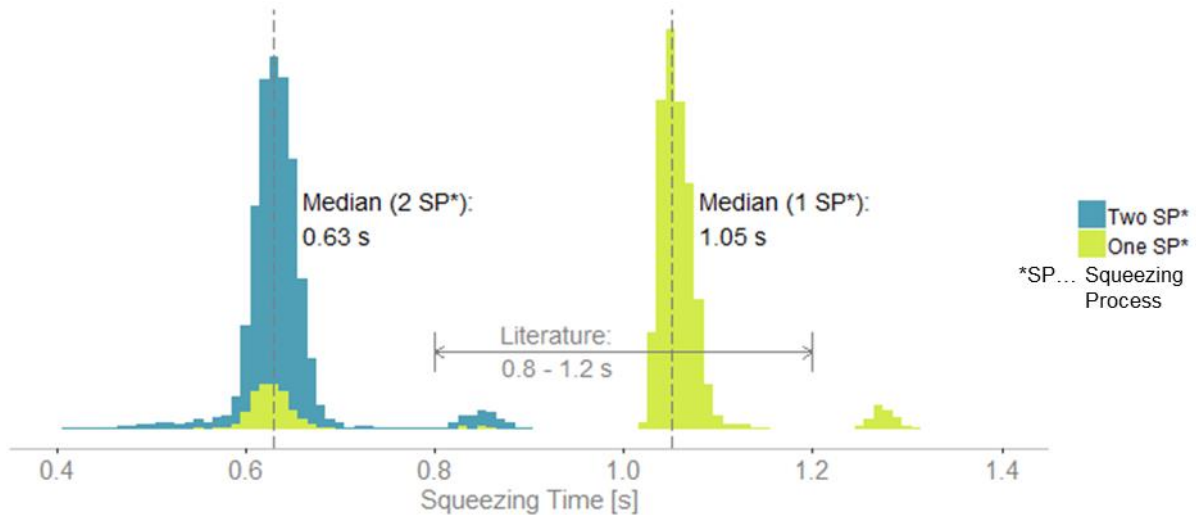
Figure 37: Recorded squeezing times

In the plot, two striking peaks at 0.63 seconds and 1.05 seconds can be identified. Whether the tamping machine was set to the lower or the higher value, mainly depends on the number of performed squeezing processes (which themselves depend on lifting height [25]). If one squeezing process was enough, the squeezing time was set to approximately 1.05 seconds and fell in the anticipated range. If two squeezing processes were required, each of them, on average, lasted about 0.63 seconds on average. During maintenance actions, the share of single and double squeezing processes was almost equal. In contrast, track renewals were almost exclusively executed with two consecutive squeezing processes.

6.2.2 Squeezing Velocity

Squeezing velocity should be 150 mm/s for sufficient energy transfer from the tamping tines into the bedding [25]. The distributions in Figure 38 indicate that this value is rarely reached in reality. With an overall median of approximately 60 mm/s, recorded squeezing velocities were about 60% below the theoretical optimum. A comparison of single and double squeezing processes shows almost equal medians. However, the distributions display different deviations. Double squeezing processes feature a larger deviation and a less

pointed peak. This can be explained by the circumstances, under which two squeezing processes were performed: either during track renewals (supposedly good ballast condition) or in areas of heavily fouled ballast (see Chapter 7.4).
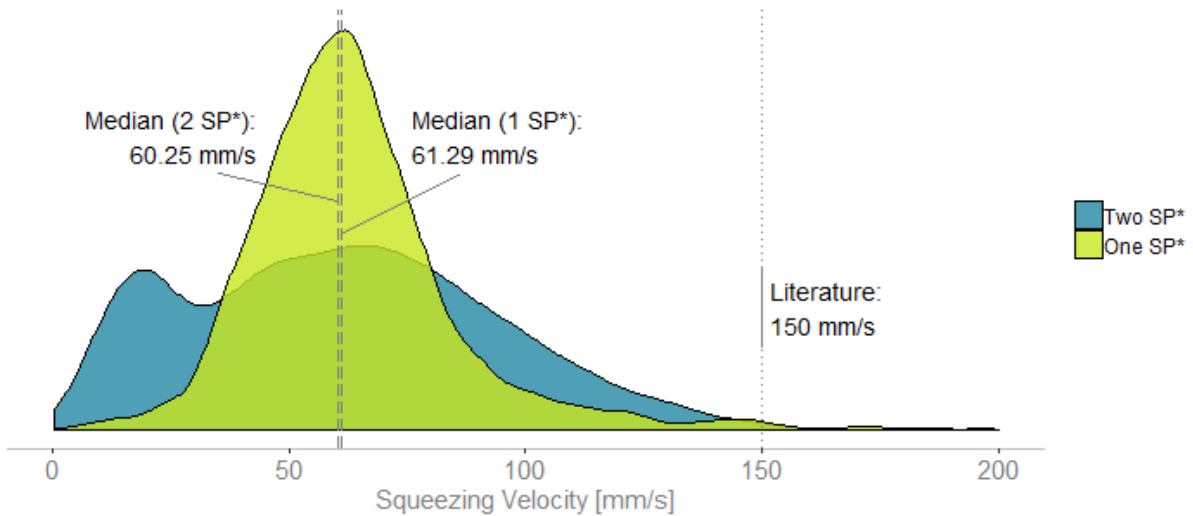
Figure 38: Recorded squeezing velocities

Assuming an oscillation frequency of 35 Hz (see Chapter 3.3.3) during the squeezing process, squeezing velocities of 60 mm/s equal an impact duration of about 3.5 ms (Figure 39). A period of at least 5 ms is desirable to guarantee efficient energy transfer and optimal tamping results [25]. This evaluation raises the question whether tamping units should be calibrated differently to reach velocities of 150 mm/s or if literature should be reconsidered.
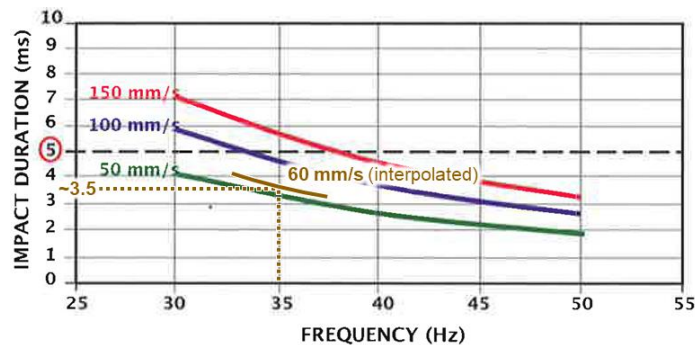
Figure 39: Influence of squeezing velocity on impact duration [25]

However, according to Plasser & Theurer, it is doubtful whether recorded velocities are trustworthy. The responsible sensor might have been biased by the tine oscillation and has recently been replaced by a different system.

6.3 Analysis of Infrastructure Data

Tamping actions analysed in this study were executed on different network sections. Naturally, they feature different track components and varying track conditions. As these factors may influence tamping measurements, this chapter gives an overview of asset data and ballast condition on the respective sections. This part of the study is limited to tamping actions on the southern line. It includes maintenance and track renewal tamping.

6.3.1 Asset Data

Relevant asset data for this study are sleeper type and sleeper age (which corresponds with ballast age). 54% of the tamping processes were maintenance actions, 46% part of track renewals. On the tamped sections, all three main sleeper types used in Austria, occur. With 48%, concrete sleepers account for the biggest share. Concrete-USP sleepers make up 33%, and the remaining 19% are wooden sleepers (Figure 40). Concrete sleepers were solely tamped during maintenance and concrete-USP sleepers exclusively during track renewals. As concrete-USP sleepers are a newer technology and deliver more durable track geometry, sections featuring this sleeper type are less likely to require realignment. On the other hand, this hints at a possible strategy pursued by ÖBB Infrastruktur AG to no longer install common concrete sleepers on main lines. Only wooden sleepers are split – some have been in place for years and some were newly installed during track renewals. Although concrete-USP sleepers would be preferable on a highly loaded line like *Südbahn*, wooden sleepers must be used in tight bends for technical reasons.
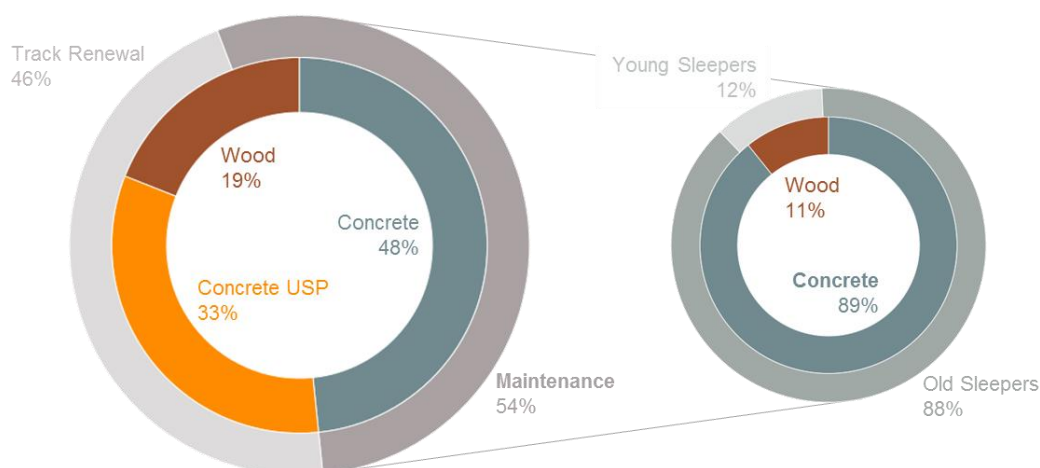
Figure 40: Portions of tamping types and sleeper types

Figure 41 provides additional information on tamped sleepers by revealing their installation year. Sleepers whose installation dates back to 2016 and 2017, were installed in the course of track renewals. Corresponding tamping actions are named *track renewal tamping*. Sleepers which were tamped during maintenance, can be divided into two groups: old concrete sleepers and young wooden sleepers. Most concrete sleepers are between 15 and 30 years old while wooden sleepers, apart from very few exceptions, are younger than 10 years. These different age groups need to be considered when evaluating ballast condition.
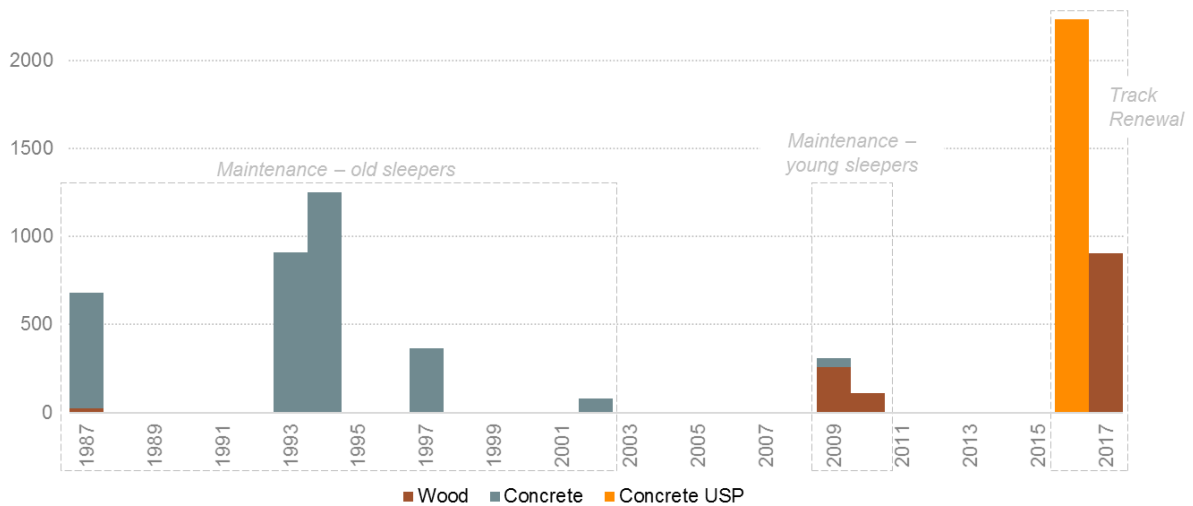
Figure 41: Installation years of the sleepers

6.3.2 Ground Penetrating Radar

Recordings of ground penetrating radar are divided into different groups. Four of them describe ballast condition: Ballast fouling, ballast humidity, clay fouling and interlayer humidity. Each category is assigned different attributes. For example, the category *Clay Fouling* can either be classified into *No clay fouling*, *Basal clay fouling* or *Clay fouling in the ballast bed*. Figure 42 reveals the apportionment of these classifications for each category. The data originate from 2013.
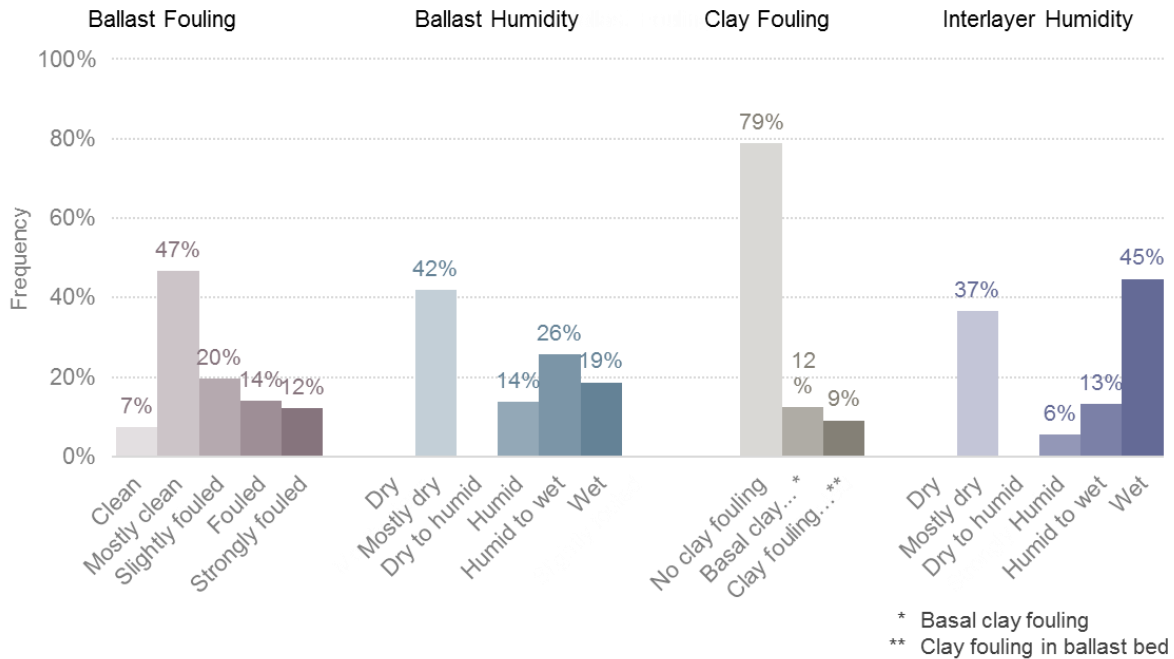
Figure 42: Ballast condition on tamped sections

More than half of the tamped sectors show no or little ballast fouling (7% and 47% respectively). The other part ranges between *Slightly* and *Strongly fouled*, with the share steadily decreasing as fouling rate rises. This distribution is very similar to an evaluation conducted on net-wide data.

Regarding humidity, ballast and interlayer show related characteristics. In both cases, a big part is *Mostly dry*. Meanwhile, the attributes *Dry* and *Dry to humid* are not present at all. A major part of the analysed sections ranges between *Humid* and *Wet*. The high percentage of wet interlayer may hint on dewatering or substructure issues. However, this parameter is not supposed to affect tamping results as the tines do not enter the ballast bed this deeply.

Clay fouling arises from lower zones and has more effect on the transition area between ballast and substructure. Higher zones are generally less effected by clay fouling. Only in 9% of the examined track, clay has already accumulated in the lower ballast bed. By and large, clay fouling is a minor issue on the analysed sections.

6.3.3 Fractal Data

Medium-wave range fractal values lie between -0.47 and -29.38 with a median value (horizontal line in the rectangle; Figure 43) of -6.14. Typically, -8.5 is considered as threshold level for ballast condition assessment [19]. Higher values are desired, lower values indicate ballast issues which should be monitored and may require action. Half of the data, marked

by the interquartile range (marked by the rectangle of a boxplot; it is confined by 25%- and 75%-quantile; see Figure 43), vary between -3.96 and -8.31. Hence, approximately three quarters of the analysed cross-sections (all values in the interquartile range plus those above the upper limit of the box) are in an acceptable condition. The boxplot in Figure 43 excludes values with magnitudes below -20. These extremely poor figures originate from a short section between Felixdorf and Wr. Neustadt, which was renewed in 2016.
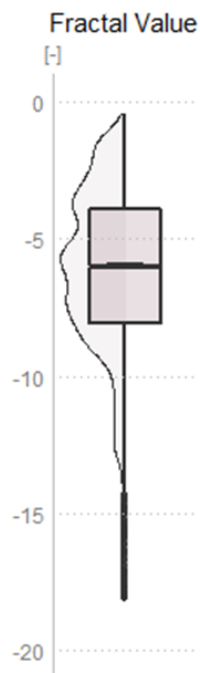
Figure 43: Distribution of fractal values

6.3.4 Ground Penetrating Radar vs. Fractal Analysis

A comparison of GPR results and fractal analyses reveals unusual disagreements between the two evaluation methods (Figure 44). There are several possible reasons for that: Both systems indirectly assess ballast condition and can be influenced by factors beyond control, e.g. weather condition. Furthermore, while the calculated fractal values represent a time series, GPR data originate from one single measurement performed in late 2013. Ballast condition has most certainly changed since then.

Only ballast humidity shows a slight downward trend in humid and wet areas. Ballast humidity mainly correlates with higher regions of the ballast bed, as do fractal values. Therefore, their connection is reasonable. This is also the area the tamping tines come in contact with, hence it is the most important GPR parameter.
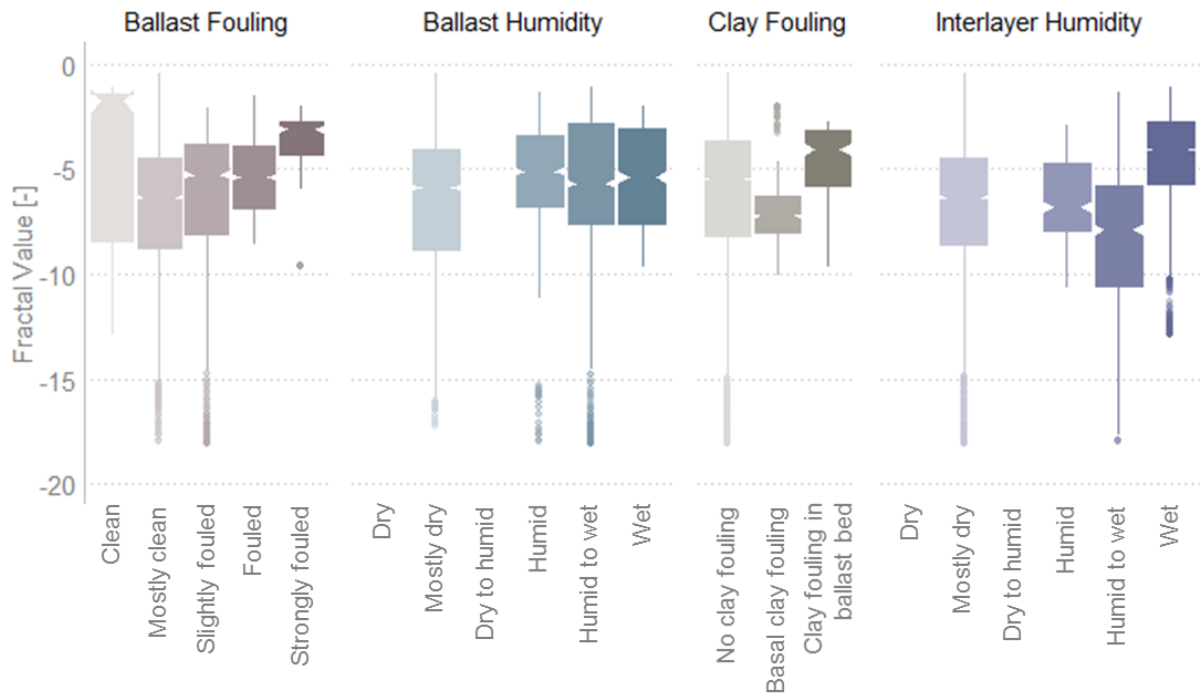
Figure 44: GPR vs. fractal analysis

To avoid the issue of weak correlation between GPR and fractal analysis, a ballast condition figure, combining results of both systems, is calculated.

6.3.5 Ballast Condition Figure

In an attempt to combine different condition evaluation methodologies to a holistic condition assessment, a ballast condition figure was established. It considers GPR data, fractal values and track alignment. Fractal analysis is the most suitable single method to describe ballast condition. Therefore, it is the biggest contributor to the ballast condition figure. [17]

In this study, a slightly modified version is applied, focusing on GPR and fractal data while excluding track alignment. The relative shares of the considered parameters, which are presented in Table 5 together with their weightings, are kept equal.

Since fractal values and GPR information become invalid when a track is renewed, this part of the study only applies to maintenance data. This also explains the maximum fractal value of -12.53 in the table below. Before the ballast condition figure is calculated, data points exhibiting installations like turnouts or bridges, are removed. They may influence the two evaluation methodologies.

Data Analysis and General Results

Evaluation methodology GPR		
Criterion	max value	Weighting ε [%]
Ballast Fouling	5	29
Ballast Humidity	6	63
Clay Fouling	3	8
Interlayer Humidity	6	0

γ = 38 %

Evaluation methodology Fractal Analysis		
Criterion	max value	Weighting ε [%]
Fractal mid-wave	-12.53	100

γ = 62 %

Condition
Figure
Ballast

Table 5: Criterions and weightings for the ballast condition figure acc. to [17]

The calculation is done according to Formula 2:

$$BZ_m = \left(1 - \sum_{i=1}^{n} \frac{N_{m,i}}{Max_{m,i}} * \varepsilon_{m,i}\right) * 100 \qquad ZZ_{Ballast} = \sum_{m=1}^{n} BZ_m * y_m$$

Formula 2: Calculation of the ballast condition figure

BZ_m *Ballast condition based on methodology m*

$N_{m,i}$ *Value of criterion i based on methodology m*

$Max_{m,i}$ *Maximum value of criterion I based on methodology m*

$\varepsilon_{m,i}$ *Weighting coefficient for ballast of criterion I based on methodology m*

γ_m *Weighting coefficient for holistic ballast condition of methodology m*

ZZ   *Condition figure*

The ballast condition figure ranges from 0% to 100%, whereupon higher values indicate better ballast condition and vice versa. 100% would be a perfectly clean and dry ballast bed. In contrast, values close to zero mark extremely poor sections. When comparing ballast condition and tamping data, the condition figure is clustered into three groups in order to obtain as distinct results as possible*: poor ballast condition, mediocre ballast condition* and *good ballast condition*. Only few points, which are rated very low by both methodologies (GPR and fractal analysis), are allocated the *poor* cluster. Likewise, points must be rated high by both evaluation methods to be marked as *good ballast condition*. The medium cluster comprises the vast majority of data.

Correlations between ballast condition and tamping data, presented in Chapter 7, are evaluated separately for concrete and wooden sleepers. This avoids a mixture of different sample sizes and age categories of the two sleeper types. For this reason, the distribution of the ballast condition figure is also divided into concrete sleepers (Figure 45) and wooden sleepers (Figure 46).
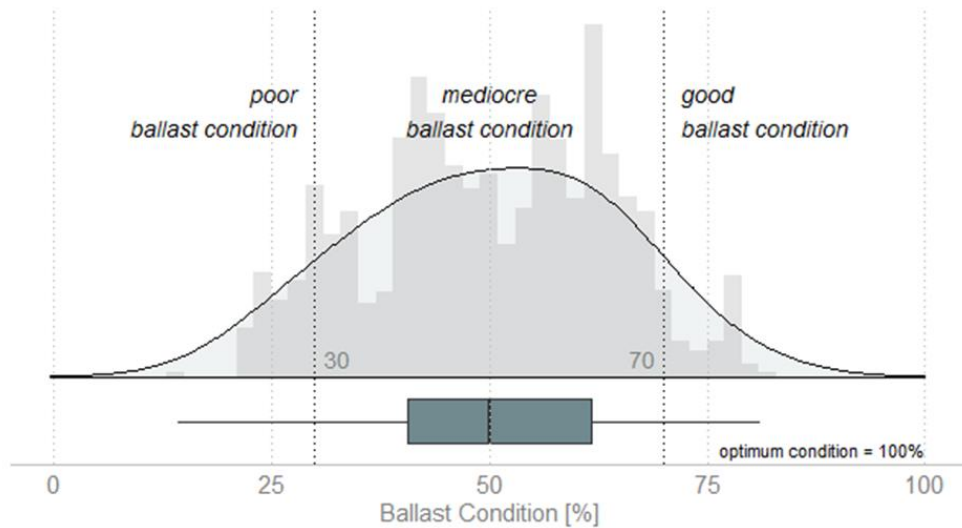
Figure 45: Distribution of the ballast condition figure (concrete sleepers)

Sections equipped with concrete sleepers exhibit a uniform condition distribution with a median value of 49.9%. The borders for the three condition clusters are set at 30% and 70%. 277 values are lower than 30% and represent poor ballast condition. 161 values show good condition with condition figures above 70%. The medium cluster comprises the remaining 2475 data points.

The ballast condition distribution for wooden sleepers shows a slightly different picture. It is less uniform and tends to higher values, e.g. better ballast condition. This may be attributed to the lower age of wooden sleepers and the elastic behaviour of the material which protects the ballast bed (see Chapter 2.1.2). The boundary confining the poor cluster is adjusted to 35%, as there are no values below 30%. Still, only 21 values undercut the adapted boarder. Meanwhile, good ballast condition again ranges from 70% to 100% and contains 46 values. The residual 255 data points represent mediocre condition.
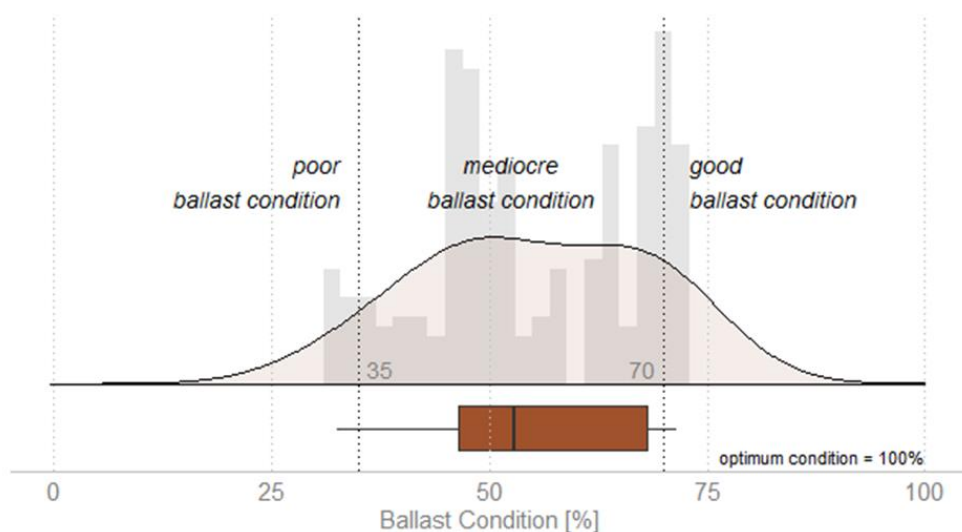
Figure 46: Distribution of the ballast condition figure (wooden sleepers)

6.4   Analysis of Tamping Data

An overview of the recorded tamping parameters is provided in form of boxplots and distributions in Figure 47. These data comprise maintenance and track renewals on the southern line. Squeezing time and values of the second squeezing process are excluded for aforementioned reasons.

Penetration Force follows a uniform distribution with a slight positive skew. Its values range between 4.61 and 56.34 kN. All other parameters do not show uniformness. Instead, *Squeezing Force* (1.38 – 29.46 kN) and *Squeezing Velocity* (0.42 – 161.26 mm/s) are widely spread and form a plateau. *Standardized Energy per Squeezing Movement* attains values between 0 and 3433 J/s. It features a unique peak at the lower end and a plateau in the upper part. *Loading Stiffness* and *Unloading Stiffness* show two peaks, indicating different behaviour of two groups in the underlying data set. This results from the two tamping types, as the next chapter will clarify.
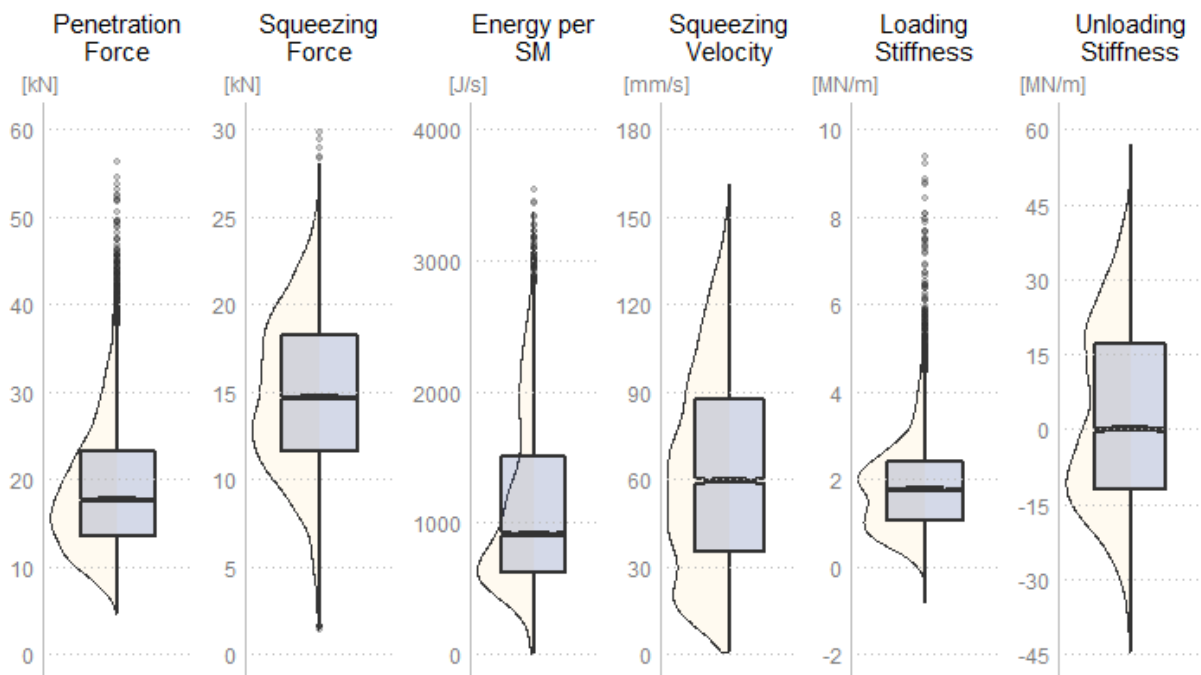
Figure 47: Overview of tamping data

Unloading Stiffness accepts positive and negative values with one peak above and one below zero. It ranges between -44.74 and +57.12 MN/m. In very few cases, *Loading Stiffness* also reveals negative values, beginning at -0.86 MN/m. Technically, this is impossible. Therefore, these are either measurement or calculation errors (stiffness values are not direct measurements, but calculated parameters based on other recordings). However, most *Loading Stiffness* values are positive and therefore reasonable, going up to 9.2 MN/m.

7 Ballast Condition Assessment via Tamping Data

As key part of this study, this chapter deals with correlations between tamping data and infrastructure data. First, measurement parameters are individually examined for different tamping types (track renewal vs. maintenance) and sleeper types. Thereafter, maintenance data are evaluated in regard to ballast condition. This step is done for concrete and wooden sleepers separately. Thus, possible influences of different sleeper types are not mixed and concrete sleepers, which comprise almost 90% of the data, are not overrepresented. Next, squeezing time, which is generally excluded (for it is not an objective parameter), is investigated regarding possible connections with ballast condition. The last part summarizes the obtained results and includes a discussion of the extracted information. Additionally, it will be assessed if different measurement parameters are suitable for ballast condition evaluation

Many evaluations shown below, make use of boxplots. A statistical way of gaining extra information from them, is drawing notches at the median line. The length of the notches depends on sample size and variation of the data. If notches of two boxes do not overlap, there is a 95% chance that the medians of both groups differ significantly. This indicates that the data represent different samples [35]. In this study, non-overlapping notches provide statistical evidence that differences in the recorded measurements can be attributed to tamping or sleeper types (Figure 48) or ballast conditions (Figure 49, Figure 50).

Discussions of the results are based on the assumption that machine settings, except for squeezing time, are always equal, regardless of the tamping type or ballast condition.

7.1 Evaluation of Tamping and Sleeper Types

Tamping actions right after track renewals are presumably executed in new, clean ballast. However, this ballast has not yet formed a stable, interlocked matrix. In contrast, ballast condition on sections which require maintenance, has supposedly degraded to a certain degree, hence triggering track work. Therefore, tamping parameters are expected to reveal differences between these two tamping types. In addition to comparing tamping types, data are also classified into sleeper types. This allows an assessment whether tamping type or sleeper type has more influence on the results and prevents commingling of different influencing factors. Therefore, four boxes are presented for each tamping parameter.

Figure 48 presents all six relevant parameters: *Penetration Force*, *Squeezing Force*, *Energy per Squeezing Movement*, *Squeezing Velocity*, *Loading Stiffness* and *Unloading Stiffness*.

The tamping type is indicated by the colour of the boxes. Bright grey stands for track renewal data and dark grey for maintenance data. Sleeper types are represented by the outline colours of the boxes. Concrete sleepers feature a grey outline, concrete-USP sleepers are orange and wooden sleepers brown. As shown in Chapter 6.3.1, concrete sleepers were only tamped during maintenance and concrete-USP solely during track renewals. Thus, only wooden sleepers occur with both fill colours (in both tamping types).
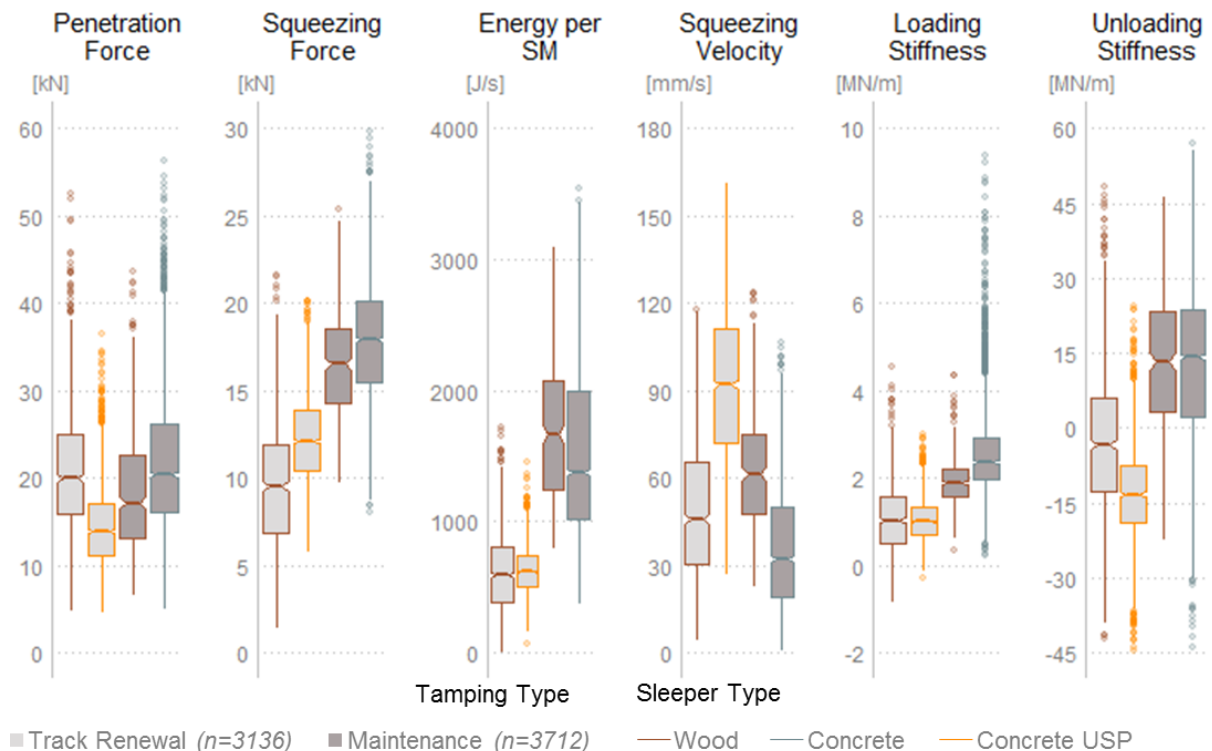
Figure 48: Tamping parameters for different tamping and sleeper types

The behaviour of *Penetration Force* is somewhat arbitrary. While the two tamping types do not show a clear difference, sleeper types seem to play an important role for this parameter. Neither the big gap of wooden and concrete-USP sleepers in track renewal data nor the similarity of track renewal wood and maintenance concrete can be explained so far.

Squeezing Force seems to depend on multiple factors. It is significantly lower during track renewals than during maintenance actions. This is probably a result of the not yet established interlocked ballast matrix, hence stones can be rearranged easier. Moreover, sleeper types reveal differences. In case of maintenance data, the higher values of concrete sleepers may be attributed to their greater age.

Energy per Squeezing Movement takes on very low levels during track renewals, which are similar for both sleeper types. Again, maintenance data are much higher and differ between sleeper material. Only this time and in contrast to the squeezing force, concrete sleepers feature lower measurement values than wooden sleepers.

Squeezing Velocity seems to heavily depend on the sleeper type. Additionally, a difference between tamping types can be noticed when observing wooden sleepers, with higher measurements during track renewals. Highest squeezing velocities are recorded on new sections featuring concrete-USP sleepers. Potentially, the soft layer on the sleeper-underside enables quicker rearrangement of the stones. As explained in Chapter 6.2.2, this parameter may not deliver reliable results due to challenges with the measuring system.

Loading Stiffness shows similarities with *Squeezing Energy* during track renewals. As with *Squeezing Energy*, medians of wooden and concrete-USP sleepers are almost equal but data of wooden sleepers vary stronger than those of concrete-USP sleepers. Maintenance data show that ballast bed stiffness of long utilized sections is much higher compared to just installed, not yet compacted ballast. Data recorded in tamping processes at concrete sleepers exhibit some very high measurements. These may result from attritions of the sleepers – such *white spots* are predestined to stiffen.

Unloading Stiffness features a distinct characteristic as it can either be positive or negative. During track renewals, the medians of both tamping types are below zero, whereas data from maintenance actions tend to be positive. However, data of both tamping types can take on positive and negative values. Regarding track renewals, sleeper types significantly differ whereas maintenance data reveal almost equal behaviour of the two sleeper types.

7.2 Evaluation of Ballast Condition (Concrete Sleepers)

With 2913 data points, concrete sleepers comprise almost 90% of recorded maintenance data. Although all data used for upcoming evaluations originate from the same line (*Südbahn*), the results are representative as tamping actions were performed on both tracks and in different areas.

Incorporating ballast condition figures between 30% and 70%, the cluster *mediocre ballast condition* (grey in Figure 49) contains most of the data and shows highest variance. For all tamping parameters, minimum and maximum fall into this cluster. The other two groups, representing good (yellow) and poor (blue) ballast condition, contain about 440 data points together. Only data points featuring definitely good or bad condition end up in the respective clusters. The boxplots in Figure 49 show the six relevant tamping parameters, separated into the three ballast condition clusters.
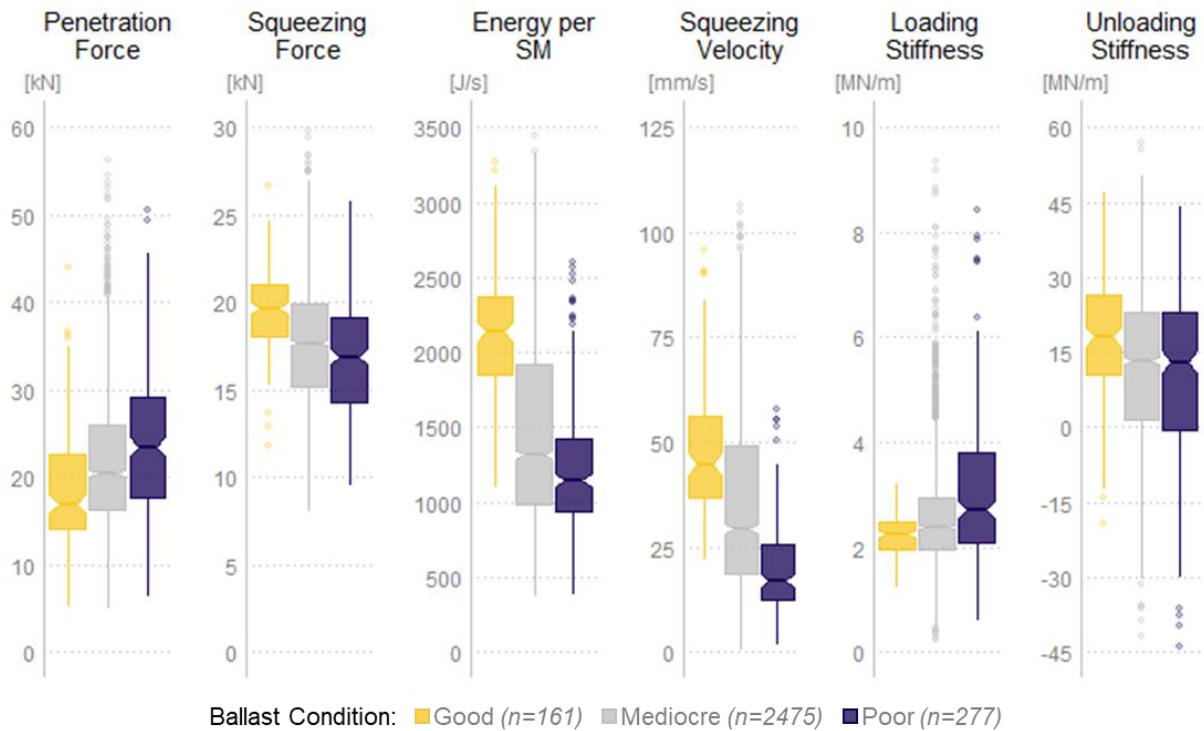
Figure 49: Tamping data in dependence of ballast condition (concrete sleepers)

All six parameters significantly differ between good and poor ballast condition, demonstrated by non-overlapping notches. The expressiveness of the results is further undermined by the mediocre cluster. The median value of all parameters lies between the other condition groups' medians. Except for *Loading-* and *Unloading Stiffness*, none of the notches overlap. Thus, the three condition clusters reveal unique trends.

An interesting aspect is the varying direction of the trends. Two parameters, *Penetration Force* and *Loading Stiffness*, increase as ballast condition worsens, while the rest decreases simultaneously. Possible reasons are discussed in Chapter 7.5.

7.3   Evaluation of Ballast Condition (Wooden Sleepers)

Wooden sleepers, tamped during maintenance, are analysed in a similar way as concrete sleepers. Again, the data are divided into good, mediocre and poor ballast condition. Only this time, the ballast condition figure separating mediocre and poor condition, was set to 35% rather than 30% (see Chapter 6.3.5). The other separator remains at 70%. The overall sample size is 322 data points, 255 of which are to be found in the middle cluster. Good ballast condition is represented by 46 values, poor condition by a sample size of 21.
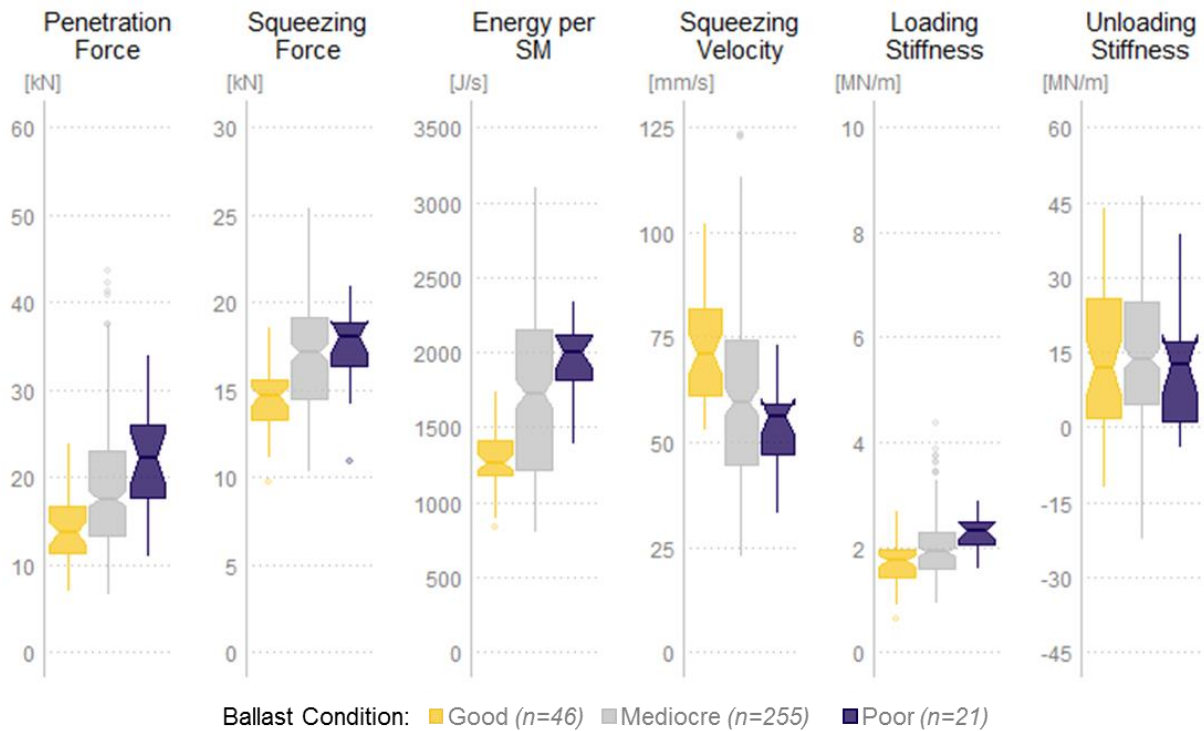
Figure 50: Tamping data in dependence of ballast condition (wooden sleepers)

Except for *Unloading Stiffness*, the results of wooden sleepers and concrete sleepers are similar in a way that they also depict significant differences between good and poor ballast condition. Due to the small sample size, the notches of the boxes are wider and partly overlap with the mediocre condition cluster.

Conspicuously, *Squeezing Force* and *Squeezing Energy* show an opposite tendency compared with concrete sleepers. To get a clue how this is possible, the underlying data need to be examined. On the one hand, the sample size of wooden sleepers is substantially lower than the one of concrete sleepers. On the other hand, all data featuring wooden sleepers originate from only two track sections, both of which are affected by different issues. Unsurprisingly, data classified as *good ballast condition* feature high fractal values and little to no *Ballast Fouling* and *Clay Fouling*, according to GPR data. However, *Ballast Humidity* and *Interlayer Humidity* values of 5 or even 6 (worst possible rating) indicate substantial dewatering issues in these areas. The opposite condition cluster (*poor ballast condition*) contains only points of one short section which, according to fractal data, should be in an acceptable condition (fractal values of -6 or higher). However, GPR ratings of this segment are catastrophic. All four categories, *Ballast Fouling*, *Ballast Humidity*, *Clay Fouling* and *Interlayer Humidity* exhibit highest possible values (equalling worst possible condition). The big discrepancy between fractal analysis and GPR evaluation is unusual. Potentially, the ballast bed was cleaned after the ground penetrating radar had evaluated this line. Yet, such maintenance is not registered in the machine deployment data. However, they could be erroneous too. No matter the cause for the discrepancy, uncertainty remains

and the results of maintenance actions on wooden sleepers should be used carefully and regarded with suspicion.

7.4 Comparison of Squeezing Time and Ballast Condition

Squeezing time is not an objective measurement parameter depending on ballast condition, but a pre-set value. For this reason, it was excluded in ballast condition analyses. However, the evaluation illustrated in Figure 51 provides a clear picture of squeezing time depending on ballast condition. Assuming machine operators do not discriminate sleeper types when setting squeezing time, concrete and wooden sleepers are mingled in this analysis. Limits for the three ballast condition clusters are set to 30% and 70% respectively.
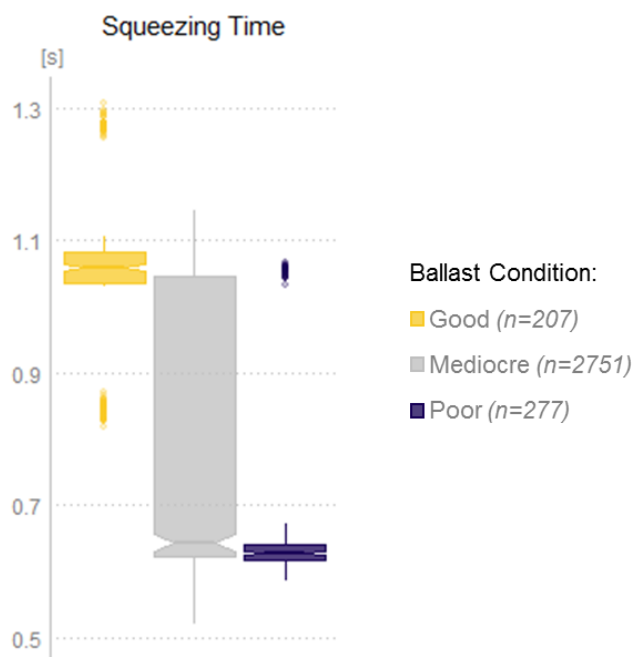
Figure 51: Evaluation of squeezing time and ballast condition

The analysis of squeezing time reveals a clear difference between ballast conditions. Sections in adequate state were squeezed for 1.05 seconds, on average. In contrast, average squeezing movement at heavily contaminated spots lasted 0.67 seconds. Considering that short squeezing time implies a second squeezing movement (see Chapter 6.2.1), two conclusions are possible: Either track alignment on heavily fouled sections was deteriorated to a level that required two lifts (equals great lifting heights), or the machinist identified poor ballast condition and chose two squeezing movements for better, long lasting results.

7.5   Summary and Discussion of the Results

Except for the non-objective *Squeezing Time*, all above presented results are clearly summarized in Table 6. Each of the six tamping parameters is described by three trend-diagrams. The first one shows if a significant difference between track renewal and maintenance tamping is discernible. The second one represents trends regarding ballast condition, extracted from maintenance data recorded on sections with concrete sleepers. The third trend-diagram summarizes the results of maintenance tamping on sections featuring wooden sleepers.

    Trend 1:   Track renewal vs. maintenance
    Trend 2: Good ballast condition vs. poor ballast condition – concrete sleepers
    Trend 3: Good ballast condition vs. poor ballast condition – wooden sleepers

Fluctuating yellow beams in Table 6 indicate that no distinct trend can be determined. Red beams, rising from left to right, show an increase of the parameter between track renewal and maintenance with increasingly poor ballast condition. Decreasing green beams indicate a decline of the recorded parameter whilst ballast contamination increases. As differences of tamping type and sleeper type have already been described in Chapter 7.1, below discussion focuses on differences between good and poor ballast condition.

Ballast Condition Assessment via Tamping Data

Table 6: Summary of the obtained trends

The summary table illustrates that most tamping parameters depend on ballast condition. Only three cases do not reveal a significant trend, two of which regard the comparison of track renewal and maintenance. These are *Penetration Force* and *Squeezing Velocity*, which seem to be stronger affected by sleeper type than tamping type (see Chapter 7.1). The third example concerns *Unloading Stiffness* on sections with wooden sleepers. It deviates strongly and the median values of all condition clusters overlap. As stated before, these particular data are not entirely reliable.

A first assumption that track renewal can be equated with good ballast condition and maintenance with fouled ballast, is not confirmed by the data. Otherwise, the relation between track renewal and maintenance would be identical to trends of *good ballast condition* versus *poor ballast condition*. Most likely, this can be explained by a different structure and arrangement of the stones: Newly installed ballast is in a loose state before it is tamped and consolidated by a dynamic track stabilizer. Thus, it offers lower resistance to compaction than older but still good ballast. Therefore, the two cannot be considered equivalent.

Penetration Force shows strong dependence of ballast condition. Both analyses on maintenance data coincide that fouled ballast requires higher axial forces (in z-direction, see Figure 27) when entering the ballast bed. This may be explained by a decline of free space in the bedding with increasing ballast pollution [36]. When tamping tines penetrate the ballast, the stones try to evade. The more voids are filled with fine grain, the more this process is hampered. The only noticeable difference between concrete sleepers compared to wooden sleepers is a generally higher level of the measurement values. This may be attributed to differences in ballast age – sections featuring concrete sleepers are, on average, about 15 years older than those with wooden sleepers. However, the big gap between wooden sleepers and concrete-USP sleepers, recorded after track renewals (see Figure 48), indicates that sleepers themselves strongly influence this parameter, too.

Squeezing Force and *Standardized Energy Consumption per Squeezing Movement* are examined together since they always exhibit similar characteristics. Due to their dependence on each other (the higher the squeezing force, the greater the area of the butterfly diagram; hence, the higher the transferred energy), they correlate very well, thus explaining the analogies. Both parameters exhibit unequivocal trends, only this time wooden and concrete sleepers point in opposite directions. As explained in Chapter 7.3, data of wooden sleepers are not entirely reliable. The analysis of concrete sleepers reveals that *Squeezing Force* and *Squeezing Energy* decline when ballast contamination increases. This may be explained by two effects: When ballast stones wear and crack, they become round and their interlocking weakens. Additional accumulation of fine grain, especially when combined with humidity, reduces shear strength between the particles. (see Chapter 2.3). When tamping tines attempt to consolidate the bedding, the ballast bed "flows" around the tines. In contrast to the penetration process, the lift of sleepers offers necessary space for the stones to escape.

Squeezing Velocity heavily varies between different sleeper types. Even when only considering track renewals with supposedly uniform ballast condition, a big gap between wooden sleepers and concrete-USP sleepers is noticeable. Furthermore, this parameter strongly depends on ballast condition. A significant drop of measurement values is discernible between good and poor ballast condition. This characteristic seems to be independent of the sleeper type, though the general level is higher for wooden sleepers than for concrete sleepers. The lower velocity when tamping more contaminated ballast may again be attributed to the higher overall density of the bedding. As mentioned before, *Squeezing Velocity* might be inaccurate due to sensor problems.

Loading Stiffness is the only tamping parameter to show three identical trends. Tamping actions conducted after the track was exchanged, deliver significantly lower stiffness values

than maintenance tamping actions. If the ballast bed is in proper condition, *Loading Stiffness* deviates very little during maintenance actions. Poor ballast, however, induces strong variations of this parameter, particularly striking on sections with concrete sleepers. Possibly, the share of humidity and water in the ballast bed is responsible for this behaviour. Dry ballast, contaminated by lots of fine grain, is known to stiffen easily. Wet spots may affect ballast stiffness conversely. Although differences between good and poor ballast condition are significant, they are not as distinct as at other parameters. This might be improved by adjusting the determination of this parameter, e.g. by adapting the considered part of the butterfly diagram (see Figure 28).

Unloading Stiffness is the least consistent of the analysed parameters. Track renewals and maintenance tamping actions feature distinct differences, the median of the former one being negative and the latter one positive. Evaluations with concrete sleepers indicate a downward trend of this parameter as ballast condition worsens. However, the difference between good and poor condition is only just significant. Comparing mediocre and poor clusters, there is almost no difference at all. Regarding wooden sleepers, unloading stiffness does not show a tendency. Good and poor ballast condition feature almost identical median values while the medium cluster is slightly, but not significantly, higher. Of all analysed parameters, *Unloading Stiffness* seems least suitable to identify ballast condition.

7.6 Parameter Suitability for Ballast Assessment

Most parameters depend on ballast condition and show significant differences between good and poor sections. However, not all of them are equally suitable to assess the bedding. Due to varying deviations, some parameters represent the condition more distinctly than others. A scatter matrix (Figure 52) plots the six parameters against each other, clustered into the same groups as before (good – mediocre – poor | yellow – grey – blue). The x-axis represents the parameter of the respective row, the y-axis the parameter of the respective column.
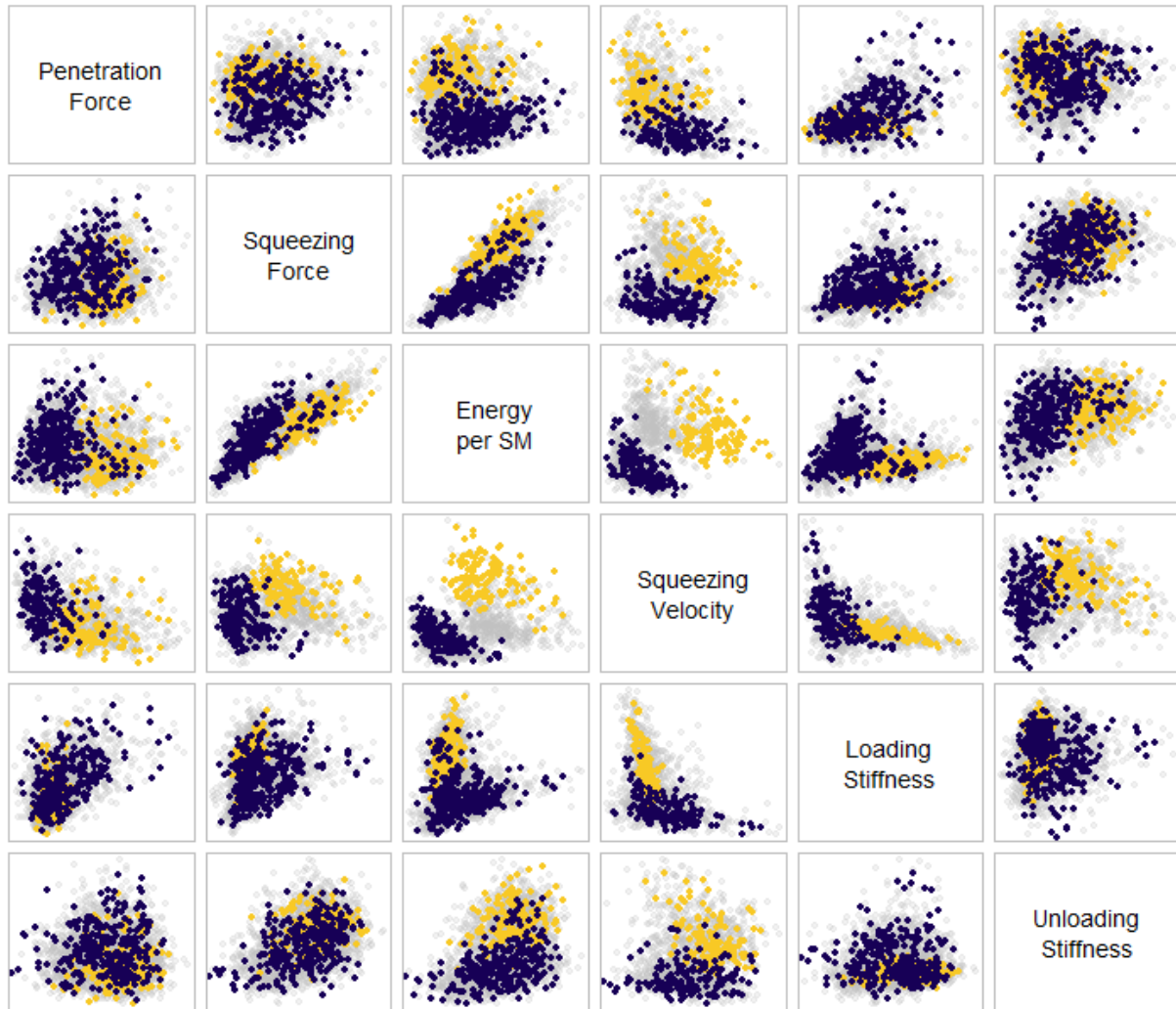
Figure 52: Scatter matrix of tamping parameters, clustered into ballast conditions (concrete sleepers)

Almost all coloured points overlap in some areas, showing that a strict distinction of ballast condition, based on these parameters, is impossible. The parameters vary too much to separate different ballast conditions. However, the combination of *Squeezing Energy* and *Squeezing Velocity* seems promising as it could clearly segregate good and poor condition. Considering the question mark behind *Squeezing Velocity*, *Squeezing Energy* is, as far as this study can assess, most suitable for ballast condition evaluation.

The same analysis is performed for maintenance data, recorded on sections with wooden sleepers, too. A smaller sample implicates that there are fewer data points. Nonetheless, yellow and blue points (good and poor ballast condition) at least partly overlap in every plot (Figure 53).
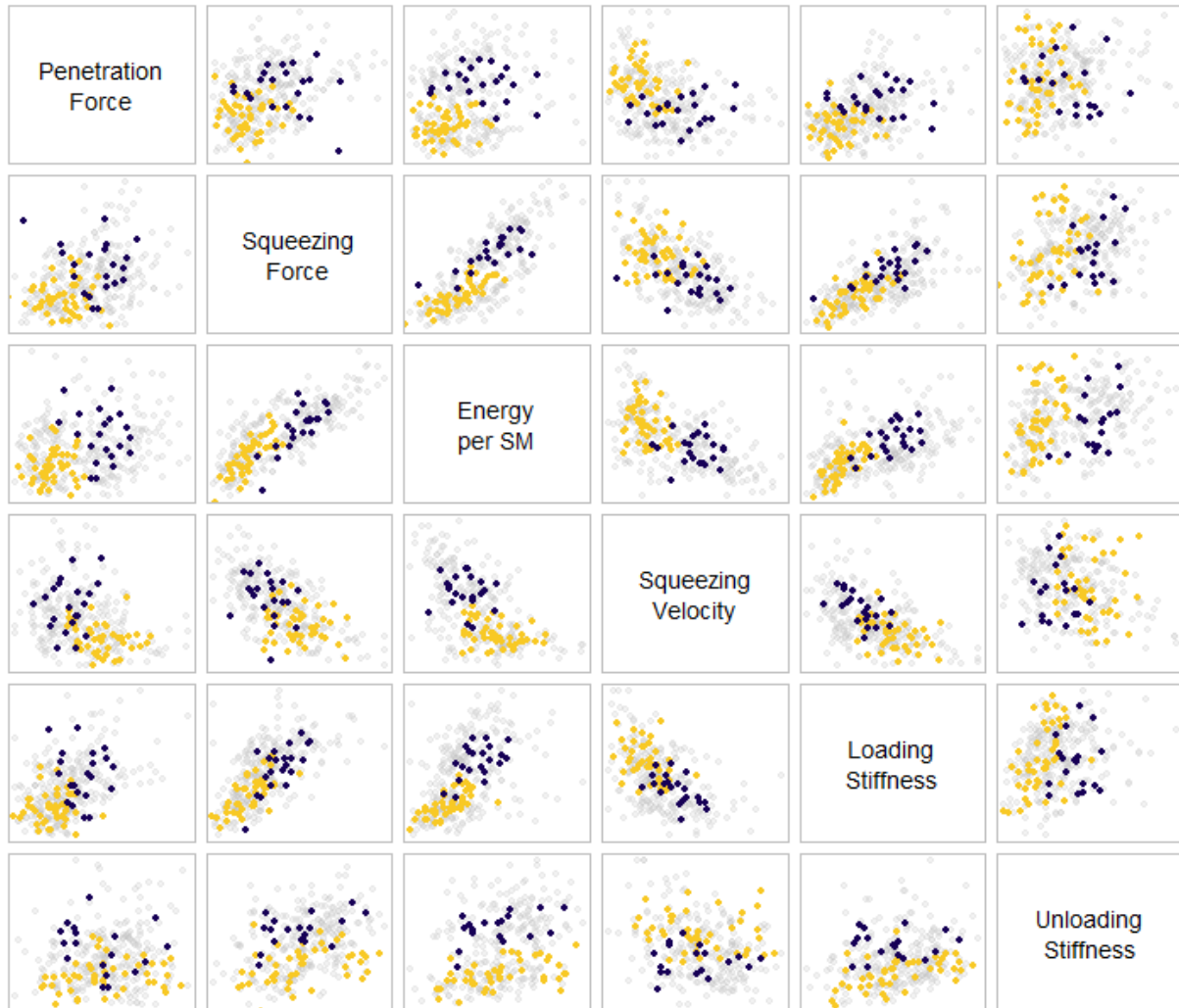

Figure 53: Scatter matrix of tamping parameters, clustered into ballast conditions (wooden sleepers)

This time, no parameter-mix enables a clear separation of good and poor ballast condition. This may partly be attributed to the dubious underlying data. However, since reliable data on concrete sleepers also struggle to separate the conditions, this is most likely not the only reason.

8 Conclusion and Prospects

During 13 tamping actions, executed in 2016 and 2017, sensors on a tamping machines' tines recorded multiple parameters. Seven of them, *Penetration Force*, *Squeezing Force*, *Energy per Squeezing Movement ("Squeezing Energy")*, *Squeezing Velocity*, *Squeezing Time*, *Loading Stiffness* and *Unloading Stiffness* are analysed in this study and connected to infrastructure data. This linkage enables comparisons of machine recordings with asset data and information on track condition. *Squeezing Time* is excluded from most evaluations and evaluated separately, as it is not an objective measurement parameter but rather an adjustable machine setting.

To obtain most reliable outputs, a ballast condition figure is calculated for every metre of the tamped sections. Merging data of ground penetrating radar (GPR) and fractal analyses, this figure offers a holistic assessment of ballast condition via a single value. Determined condition figures for the respective track sections are clustered into three groups, representing good, mediocre and poor ballast condition.

An evaluation of the recorded parameters concerning the type of tamping action, track renewal or maintenance, reveals unique differences between the two tamping types in some tamping parameters. *Squeezing Force*, *Squeezing Energy*, *Loading Stiffness* and *Unloading Stiffness* are significantly lower when tamping action takes place immediately after ballast and track grid were exchanged. In this state, the ballast is assumed to be only a loose pile of rocks rather than a stable, interlocked arrangement of stones. This could explain the deviation of the measurements from maintenance data. *Penetration Force* and *Squeezing Velocity* show greater variation between sleeper types than tamping types.

Data recorded during maintenance actions are investigated for correlations with ballast condition. Most maintenance tamping processes were performed on sections featuring concrete sleepers, making them the most reliable group. All six parameters (*Squeezing Time* is excluded) reveal unique trends and significant differences between good and poor condition of the ballast bed. *Penetration Force* and *Loading Stiffness* increase as ballast condition declines. The other four parameters follow opposite trends. *Squeezing Energy* and *Squeezing Velocity* seem most suitable for ballast condition assessment as they feature striking differences between good and poor condition.

Evaluations of maintenance data, recorded on sections with wooden sleepers, reveal partly similar, partly contrary patterns. While *Penetration Force*, *Squeezing Velocity* and *Loading Stiffness* show similar behaviour as at concrete sleepers, *Squeezing Force* and *Squeezing Velocity* trend in the opposite direction. *Unloading Stiffness*, analysed for wooden sleepers, is the only parameter not to show a trend at all. These observations need to be regarded

with suspicion, as the sample of wooden sleepers is much smaller and reliability of the underlying data is generally questionable.

Although this study was conducted with highest precision, some uncertainties remain. First, the GPS data of the tamping machine are not precise enough to identify its exact location. Therefore, all recorded positions were projected onto the nearest point on the track. Depending on the position of the GPS sensor on the machine (it is definitely near the tamping unit), an additional small error in the positioning is possible. Another factor to be considered is that the only truly reliable maintenance data originate from sections with concrete sleepers. However, it would be interesting to evaluate trustworthy recordings of tamping actions on other sleeper types, at best, from different lines all over Austria and shortly after a GPR run (to avoid comparing current tamping measurements with old ballast condition data). Furthermore, recordings of multiple tamping tines, rather than one, could be used to improve expressiveness of the conclusions. Other influences which possibly affect the results include weather condition during the tamping action, the type of rock of the ballast bed, its grain size distribution and the share of new ballast added during the tamping process. These factors could not be considered since they were (and are still) unknown. The same question mark remains concerning machine settings. Tamping machine operators can adjust numerous parameters (e.g. hydraulic pressure in the tamping unit, lifting height or tine oscillation frequency), at least some of which most certainly influence the recorded measurements. Hence, more research is advisable to validate the results of this study and amplify the understanding of the tamping process.
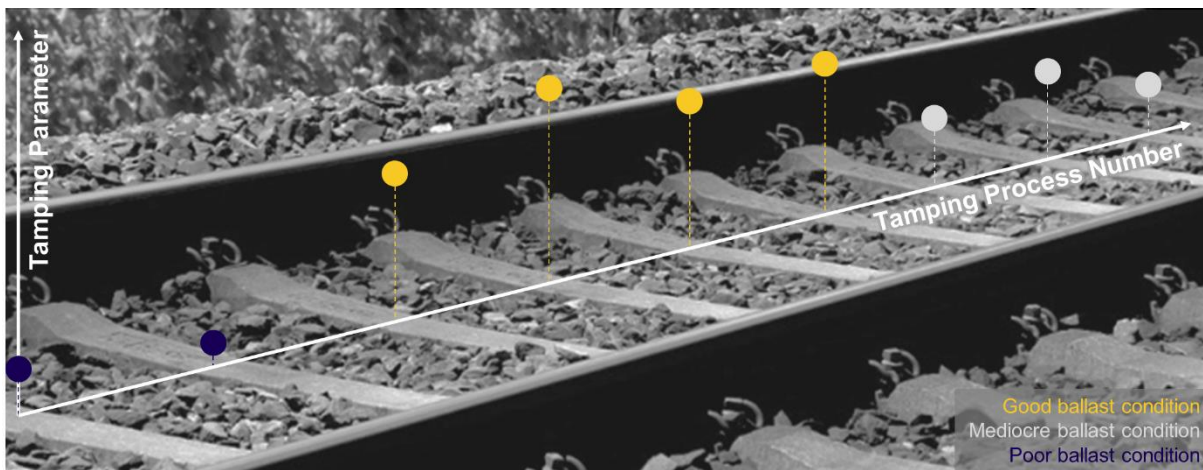
All in all, parameters recorded during the tamping actions change with ballast condition. At the moment, measurements vary too much to accurately assess the condition of the bedding by a single tamping parameter. Nevertheless, the general idea – *Ballast Evaluation as Part of Tamping Measures* – seems technically feasible.

Bibliography

[1]   B. Lichtberger, *Handbuch Gleis*, 3rd ed. Linz: DVV Media Group GmbH | Eurailpress, 2010, ISBN 978-3-7771-0400-3.

[2]   N. Avramovic, "Comparison of Ballast and Ballastless Tracks (Master´s Thesis)," Graz University of Technology, 2010.

[3]   M. Burghart, "Feste Fahrbahn: Beschreibung und Systemvergleich der Konstruktionen (Diploma Thesis)," Delft University of Technology, 2002.

[4]   S. Marschnig and M. Landgraf, "Gleisbau & -instandhaltung," Graz, 2016.

[5]   A. Berghold, "Wirkungsweise von unterschiedlichen Gleisschotterarten mit und ohne Schwellenbesohlungen," *ZEVrail*, vol. 1–2, no. A20420E, pp. 45–52, 2016.

[6]   S. Freudenstein, N. Ahmad, and D. Iliev, "Die Kontaktspannung zwischen elastisch besohlten Schwellen und Schotter," *ETR - Eisenbahntechnische Rundschau*, no. 05, pp. 13–20, 2011.

[7]   J. Neuhold and M. Landgraf, "Effects of under-sleeper-pads on long-term track quality behaviour," in *Road and Rail Infrastructure V*, 2018, vol. 5, pp. 675–681.

[8]   P. Veit and S. Marschnig, "Technische und wirtschaftliche Aspekte zum Thema Schwellenbesohlung - Teil 2: Wirtschaftlichkeit im Netz der ÖBB," *ZEVrail*, vol. 133, no. 11–12, pp. 436–443, 2009.

[9]   E. Klotzinger, "Der Oberbauschotter - Teil 1: Anforderungen und Beanspruchung," *ETR - Eisenbahntechnische Rundschau*, no. 01+02, pp. 34–41, 2008.

[10]   P. Veit, "Eisenbahnwesen Grundlagen 1 - Vorlesungsskriptum," Graz, 2018.

[11]   A. Berghold, "Wirkungsweise des Schotters im Gleis unter verschiedenen Randbedingungen (Dissertation)," Graz University of Technology, 2016.

[12]   E. Klotzinger, "Der Oberbauschotter - Teil 2: Qualitätsverlauf und Eingriffsschwellen," *ETR - Eisenbahntechnische Rundschau*, no. 03, pp. 120–125, Mar. 2007.

[13]   R. De Bold, "Non-Destructive Evaluation of Railway Trackbed Ballast (PhD Thesis)," University of Edinbrugh, 2011.

Bibliography

[14] R. Roberts, J. Rudy, I. Al-Qadi, E. Tutumluer, and J. Boyle, "Railroad Ballast Fouling Detection Using Ground Penetrating Radar – A New Approach Based on Scattering from Voids," *9th European Conference on Nondestructive Testing*, p. 8p, 2006.

[15] T. R. Sussmann, E. T. Selig, and J. P. Hyslip, "Railway track condition indicators from ground penetrating radar," *NDT & E International*, vol. 36, no. 3 SPEC., pp. 157–167, 2003.

[16] J. Niessen, "Einsatz des GeoRail®-Verfahrens von GBM Wiebe Gleisbaumaschinen für die Qualitätskontrolle nach Neu- und Umbaumaßnahmen," *DGZfP-Berichtsband*, no. 12, 2006.

[17] M. Landgraf, *Smart data for sustainable Railway Asset Management*. Graz: Verlag der Technischen Universität Graz, 2018, DOI 10.3217/978-3-85125-569-0.

[18] F. Hansmann and M. Landgraf, "Wie fraktal ist Eisenbahn? Fractal Analyses and their use in railway engineering," *ZEVrail*, vol. 137, no. 11–12, pp. 462–470, 2013.

[19] J. Neuhold and M. Landgraf, "Schotterbettreinigung als Instandhaltungsmaßnahme?," *ZEV*, vol. 140, no. 6–7, pp. 232–238, 2016.

[20] "Neue Gleise-Stopfmaschine," *Schweizerische Bauzeitung*, vol. 69, no. 3, p. 36, 1917.

[21] R. L., "Geleisestopf-Maschine System «Scheuchzer»," *Schweizerische Bauzeitung*, vol. 111/112, no. 18, p. 234f, 1938.

[22] F. Auer, R. Hauke, and R. Wenty, "High-Tech-Stopfaggregate für nachhaltige Gleislageverbesserung," *EI - Der Eisenbahningenieur*, no. 11, pp. 18–22, 2015.

[23] R. Wenty, "Kontinuierliche Gleisdurcharbeitungstechnologie im internationalen Vergleich," *Eisenbahn Ingenieur Kalender*, pp. 63–75, 2016.

[24] (Plasser & Theurer), "Kontinuierliche Gleisdurcharbeitungstechnologie im internationalen Vergleich," in *Drei Jahrzehnte kontinuierlich arbeitende Stopfmaschinen - Der Weg zu höheren Stopfleistungen.*, 2014.

[25] L. Zaayman, "Chapter 6 - Track Lifting, Levelling, Aligning and Tamping," in *Mechanisation Of Track Work In Developing Countries*, 1st ed., 2003, pp. 136–165, ISBN 978-0-620-56289-8.

[26] (Plasser & Theurer), "Der nächste Schritt - die Hybridmaschine." [Online]. Available: https://www.plassertheurer.com/de/maschinen-systeme/stopfung-dynamic-stopfexpress-09-4x-e3.html. [Accessed: 07-Feb-2019].

[27] Trackopedia & Trimble Railway GmbH, "Pre-Measuring for Tamping." [Online]. Available: https://www.trackopedia.info/lexikon/gleisbau-und-instandhaltung/gleisvermessung/vormessen/. [Accessed: 24-Jan-2019].

[28] (Plasser & Theurer), "Faster to higher quality: Levelling, lifting, lining and tamping machines." [Online]. Available: https://www.plassertheurer.com/en/machines-systems/tamping.html. [Accessed: 07-Feb-2019].

[29] K. Rießberger and R. Wenty, "40 Jahre 'dynamische Gleisstabilisation,'" *Eisenbahn Ingenieur Kalender*, pp. 55–76, 2015.

[30] R. Wenty, "Neuentwicklungen für die Fahrweginstandhaltung," *Der Eisenbahningenieur*, no. 05, pp. 44–49, 2013.

[31] O. Barbir, D. Adam, F. Kopf, J. Pistrol, F. Auer, and B. Antony, "Development of condition-based tamping process in railway engineering," *Ce/Papers*, vol. 2, no. 2–3, pp. 969–974, 2018.

[32] S. Glen, "Statistics How To," 2019. [Online]. Available: https://www.statisticshowto.datasciencecentral.com/probability-and-statistics/correlation-coefficient-formula/#Pearson. [Accessed: 17-Feb-2019].

[33] University of Cambridge, "Lost but lovely: the haversine," 2017. [Online]. Available: https://undergroundmathematics.org/trigonometry-triangles-to-functions/lost-but-lovely-the-haversine. [Accessed: 09-Feb-2019].

[34] H. Lee, "Outlier detection in Datadog: A look at the algorithms," 2015. [Online]. Available: https://www.datadoghq.com/blog/outlier-detection-algorithms-at-datadog/. [Accessed: 17-Feb-2019].

[35] J. M. . Chambers, W. S. . Cleveland, B. Kleiner, and P. A. Tukey, "Notched Box Plots," in *Graphical Methods for Data Analysis*, P. J. Bickel, W. S. Cleveland, and R. M. Dudley, Eds. Boston, 1983, pp. 60–63.

[36] H. Bach, "Evaluation of attrition tests for railway ballast (Dissertation)," Graz University of Technology, 2013.